Studies on Transition Metal Salt Dispersed poly (vinylidene fluoride) Composite films

A

Thesis

Submitted in the partial fulfilment of requirement for the degree of

MASTER OF TECHNOLOGY

In

MATERIALS AND METALLURGICAL ENGINEERING

By

SUMIT BHARDWAJ

(600802021)

UNDER THE SUPERVISION OF

Dr. K. K. Raina

School of Physics and Materials Sciences

Thapar University, Patiala, (Punjab)

June-2010

CERTIFICATE

This is to certify that the thesis entitled **"Studies on Transition metal salt dispersed poly (vinylidene fluoride) (PVDF) composites films"** submitted by **SUMIT BHARDWAJ** in the partial fulfilment of the requirement for the award of the degree of **M.Tech.** in **Material and Metallurgical Engineering** from the School of Physics and Materials Sciences, Thapar University, Patiala, is a record of candidate's own work carried out by him under my supervision and guidance. The experimental matter embodied in this report has not been submitted in part or full to any other university or institute for the award of any degree.

Dr. K.K. Raina
Deputy Director,
Distinguished Professor,
Thapar University, Patiala

Dr. O.P. Pandey
Professor and Head,
Thapar University,
Patiala, Punjab.

Dr. R.K. Sharma
Dean, Academic Affairs
Thapar University,
Patiala, Punjab.

ACKNOWLEDGMENT

I am submitting my thesis report and this work would not have been accomplished without the support, help and guidance of a large number of people.

With deep sense of gratitude I wish to express my sincere thanks to my supervisor **Dr. K. K. Raina**, **Distinguished Professor and Deputy Director, School of Physics and Materials Science,** for their excellent guidance and support throughout my work. Their unique inimitable style has left an indelible impression on me. Their constant encouragement helps and reviews during the course of Investigation are invaluable. Nevertheless it helps me acquire and develop some of the skills and intricacies of good independent research. I thank him for his great patience, constructive criticism and myriad useful suggestions apart from invaluable guidance to me.

I am grateful to **Dr. O.P. Pandey, Professor and Head, School of Physics and Materials science** for his encouragement and execution of thesis work.

I would also like to thank **Dr. Kulvir Singh, Associate Professor and PG Incharge, School of Physics and Materials Science** for his constant guidance and encouragement.

I am also thankful to all the faculty members of School of Physics and Materials Science, for their constructive suggestions at different stages of my work.

It gives me immense pleasure to express my special thanks to **Mr. Ravi Shukla (Ph.D. scholar)**, who always took keen interest in guiding me during my work. I wish to express my warm and sincere thanks to **Miss Shikha Kapila (Ph.D. scholar)**, **Miss Neeraj Sharma (Ph.D. scholar)** and my colleagues **Ishan Choudhary, Sunita Mehta, Pankaj Chamoli and Paramjyot Kumar Jha** for their support and their timely help and valuable discussions.

I owe my sincere thanks to all the staff members of School of Physics and Materials Science for their support and encouragement. Last but not the least; I would like to thank all my family members and friends for their moral support that kept my spirit up during the endeavour.

SUMIT BHARDWAJ

ABSTRACT

Pure and transition metal salt (TMS) dispersed Poly (vinylidene) fluoride PVDF composite films were derived via mixed solvent systems. The composite films loaded with varying concentrations of TMS ($CuCl_2$, $NiCl_2$and $ZnCl_2$) 0.5, 1, 3, 5, 10, 15,25wt% has been prepared. The chemical, structural, physical, morphological thermal and dielectric properties were studied by using Fourier transform infrared spectroscopy, X-Ray diffraction, Scanning electron microscopy, differential scanning calorimetery and LCR meter (50Hz to 1 MHz). IR spectra and XRD analysis collectively inferring about the formation of crystalline β-phase for all concentration of TMS. The conductivity measurement inferring that the metal salt content was well percolated in the PVDF matrix as the conduction of these composite films become higher with the rise in metal salt content. Highly ordered spherulites grown in the TMS-PVDF composite films were noticed. The $CuCl_2$ and $ZnCl_2$ based films were found more porous than that of $NiCl_2$ based composite films. Calorimetric transitions demonstrated only on endotherm peak in all cases attributed to the melting transitions of the PVDF. The entropy was found minimum in case of $CuCl_2$ loaded films and increases for $NiCl_2$ and $ZnCl_2$ systems respectively. The dielectric behaviour of these composite films does not reflecting any significant change as the magnitude of the dielectric was found same as pure PVDF.

DEDICATED

TO

ALMIGHTY GOD

&

MY LOVING

PARENTS

CONTENTS

LIST OF FIGURES

CHAPTER 1

INTRODUCTION

Several of our technologies in modern life need materials with unusual combinations of properties that cannot be met by conventional materials. This is especially true of advanced materials that are desired for aerospace, underwater, and transportation applications. For instance, aircraft engineers are working towards composite materials that have low density, are strong, stiff, and abrasion and impact resistance, and are not easily corroded; all these traits representing a difficult combination of characteristics. Advanced materials in which the polymer is the matrix with various kinds of nanoinclusions represent a new area of materials development, and opens up wide possibilities for contributions to science and technology.

In today's world polymers play a very important role in numerous fields of everyday life due to their advantages over conventional materials (e.g. wood, clay, metals) such as lightness, resistance to corrosion, ease of processing, and low cost production. Besides, polymers are easy to handle and have many degrees of freedom for controlling their properties. Further improvement of their performance, including composite fabrication, still remains under intensive investigation. The altering and enhancement of the polymer's properties can occur through doping with various nano-fillers such as metals, semiconductors, organic and inorganic particles, transition metal halides and fibres, as well as carbon structures and ceramics **[1].** Such additives are used in polymers for a variety of reasons, for example: improved processing, density control, optical effects, thermal conductivity, control of the thermal expansion, electrical properties that enable charge dissipation or electromagnetic interference shielding, magnetic properties, flame resistance, and improved mechanical properties, such as hardness, elasticity, and wear resistance.

Today's technology is the miniaturization of the electronic, actuating, sensing, linear and non linear optical devices. In the field of polymer science, piezoelectric and ferroelectric polymers play a very important role, as these polymers have applications in the field of microwave modulation, nonlinear optical properties, infrared to visible converter, electromagnetic wave, gas, temperature and pressure sensor. It is non rejectable in human tissues; there it has important medical applications **[2].** The existence of piezoelectric

polymers has been known since 1924. However, the early known piezoelectric polymers did not receive much attention because of their weak electro-mechanical response. Electroactive materials have been the primary source of actuation for Smart Devices. Numerous applications have been reported, including ultrasonic and undersea sonic techniques, robotics, vibration isolation and manipulation. The basic property of the materials used for these applications is the strain response induced by an electric field, and vice-versa. So far, most of the electroactive materials used for these applications are electroactive ceramics. However, recently it has been found that polymers, such as polyurethane and Polyvinylidene fluoride (PVDF) polymer, can exhibit very large electrostrictive and piezoelectric effects. The PVDF has been shown to exhibit relatively large elastic modulus. The PVDF exhibits the highest elastic energy of all electroactive materials, even considering ceramics and single crystal inorganic materials.

A growing interest starts after the work by Fukada in the 1950's and 1960's, which is the discovery that rolled films of polypeptides and numerous other polymers induce surface charges when stressed. A major milestone in this field was recorded with Kawai's discovery of the strong piezoelectric effect in polyvinylidene fluoride (PVDF) in 1969. Later, other PVDF co-polymers were also reported to be piezoelectric, including P (VDF-TrFE) and P (VDF-TFE).

By adding different type of additives we can modify significantly the structure and physical properties of the polymers. Some methods which are used to modify the properties of ferroelectric polymers normally induce undesired structural deformation or structural limitations which may not be feasible for a few applications such as in sensors and memory devices, and hence require a different, yet simple and cost effective approach to improve the structure and physical properties **[3].**

The metal halides fillers modify significantly the structure and physical properties. Some of the reasons for using metal salts are cost-effective processing with simple methodology (for solution cast films) and removal of metal salts by washing the films in de ionized water **[3].**

1. Polyvinylidene fluoride:

PVDF is also known as poly (1, 1-difluoroethlene) with a repeat unit (CH_2-CF_2). It is a highly non-reactive and pure thermoplastic fluoropolymer. It is also known as **KYNAR**, **HYLAR** or **SYGEF**.

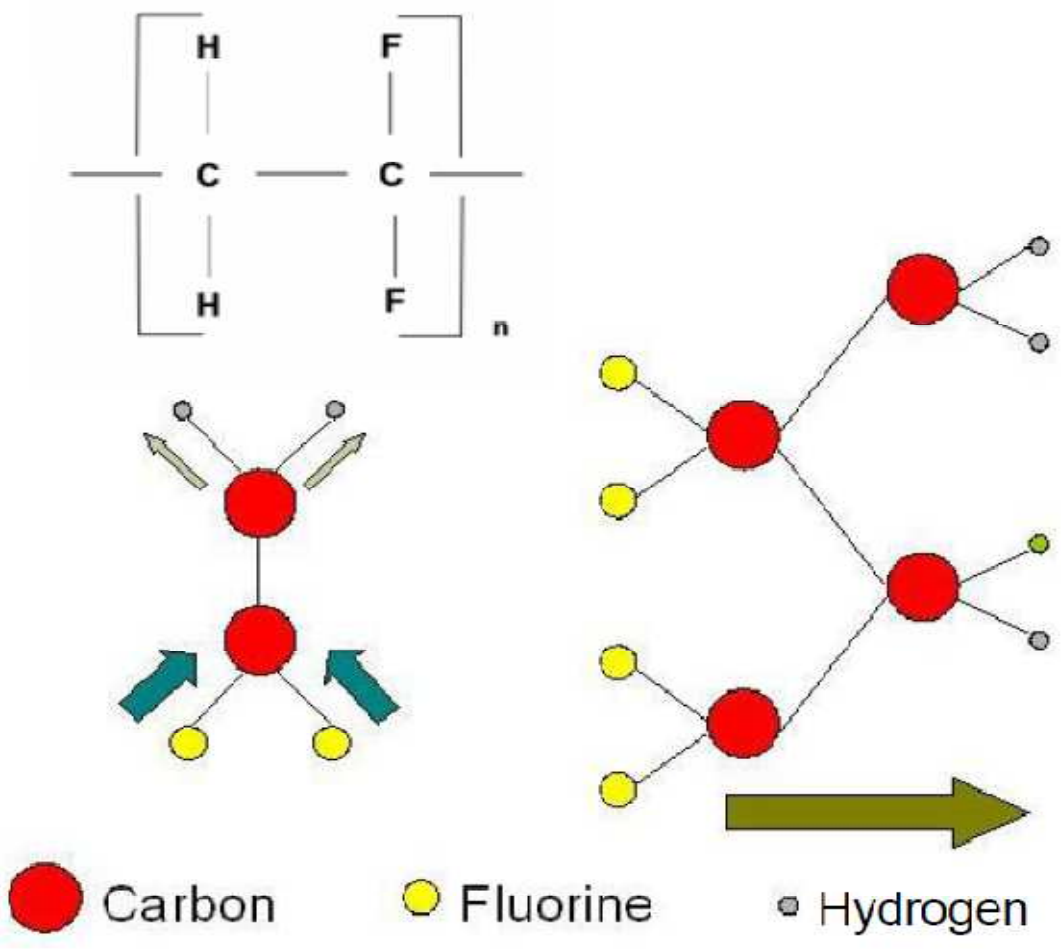

Figure 1.1: Chemical structure of PVDF

PVDF was discovered as part of Dupont's research on fluoropolymers. Polyvinylidene Fluoride (PVDF) was polymerized for the first time in the 1940s. It is usually produced by free radical polymerization of $CH_2 = CF_2$ under high temperature and high pressure, (50 to 150°C) and (10 to 300 atm); respectively. The catalysts, which are usually used, are either inorganic or organic peroxides. The breakthrough came in 1969, when Kawaii discovered the exceptional piezoelectric behavior of PVDF, which at that time was the highest among the known synthetic polymers. After more than 30 years of study and development, the piezoelectricity and electromechanical properties of PVDF and its copolymers have been

improved significantly. Today, this class of polymer still possesses the highest electromechanical responses over a broad temperature range among known synthetic organic materials and it is the only commercially available piezoelectric polymer.

1.1 Structure of PVDF

Poly (vinylidene fluoride) (PVDF) is a semicrystalline polymer with a crystallinity of about 50%,with at least four crystalline phases, α, β, γ and δ, which differ both in lattice type and chain conformation in the lattice which are stable at room temperature and three of these phase have net dipolar moments, the β phase being dominant **[4].**

α-Phase

This is the most common form of PVDF and is normally obtained by crystallization from the melt. The α-phase has a monoclinic lattice. The conformation of this phase is a slightly distorted TG+TG- with a unit cell that is non-polar due to the anti parallel packing of the two chains contained in the cell.

β- Phase

This is the most important polymorph of PVDF because this phase is predominantly responsible for the piezoelectric and pyroelectric properties of the polymer. It has an orthorhombic structure. It has an all T configuration and a strong dipole moment normal to the chain direction. It is formed by the mechanical deformation of the melt-crystallized α – phase films and the formation is aided by head-to-head ($-CF_2-CF_2-$) and tail to tail ($-CH_2-CH_2-$) defects, which help to reduce intermolecular strain.

γ- Phase

This phase is formed by solution crystallization and readily transforms into β-phase on mechanical distortion. It has an orthorhombic lattice. A number of arrangements have been suggested for this polymorph, and the T3GT3G configuration is generally accepted. It is thus seen as an intramolecular mix of both α and β forms.

δ- Phase

This is a polar α form and is produced by subjecting the α-phase to a high electric field, thus producing an inversion of the dipole moments in alternated chains. It has an orthorhombic lattice. The unit cell dimensions and the configuration are the same as the α-phase.

Because of the strong electronegativity of fluorine atoms compared to those of hydrogen and carbon, each PVDF chain possesses a dipole moment perpendicular to the polymer chain. If

the polymer chains pack in crystals with parallel dipoles, the crystal possesses a net dipole moment, as in the polar form β, γ, and δ-phases; whereas, with antiparallel chain dipoles, the net dipole moment vanishes as in the nonpolar α-phase.

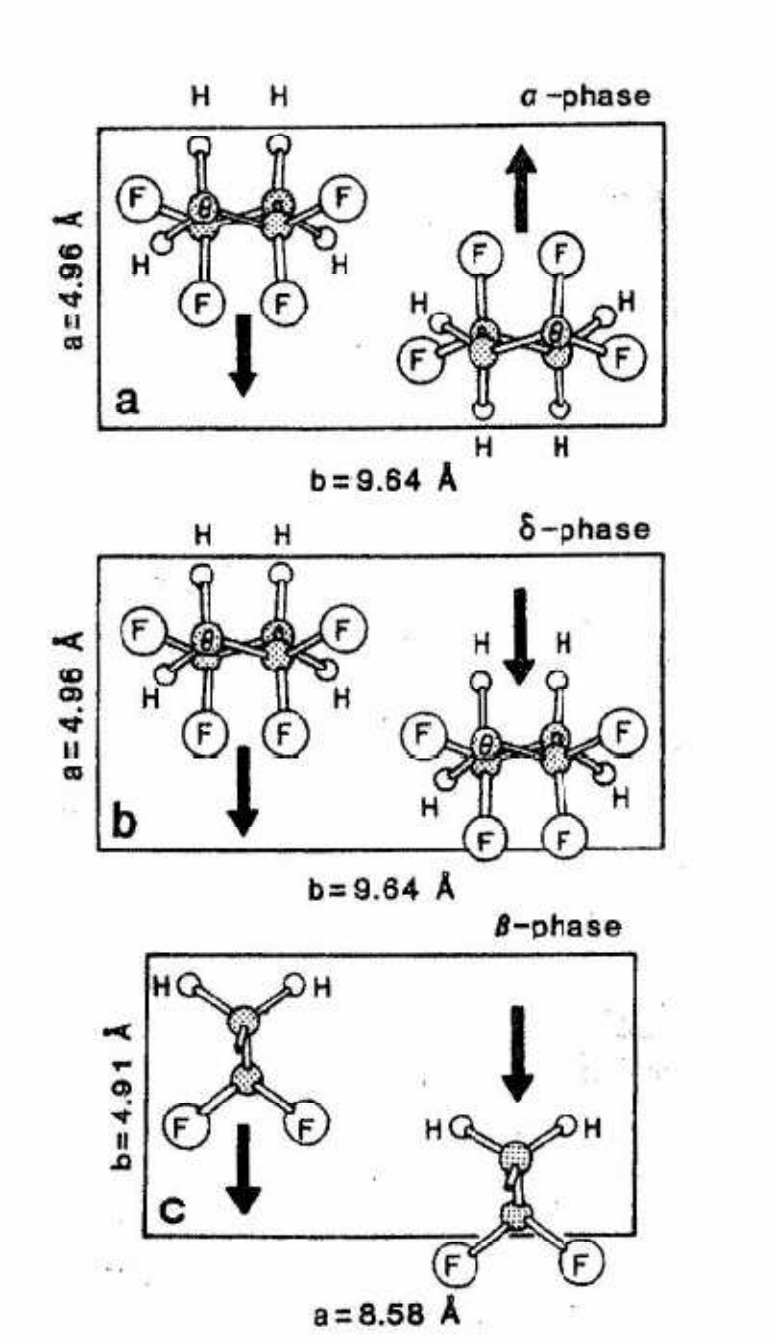

Figure 1.2: Unit cells of (a) α-phase; (b) δ-phase; and, (c) β-phase of PVDF. Only the a-b Unit-cell plane is shown. Arrows indicate dipole directions normal to molecular axis.

Among these phases, the β-phase contains the largest piezoelectric and pyroelectric coefficient. Its piezoelectricity and pyroelectricity properties, which provide possibilities for

many technological applications, have attracted much attention and have been extensively investigated over the past several decades. Currently, its copolymer—poly (vinylidene-fluoride–trifluoroethylene) [P(VDF-TrFE)] has been effectively applied as an electroactive polymer; its ferroelectricity arises from the all-trans conformation.

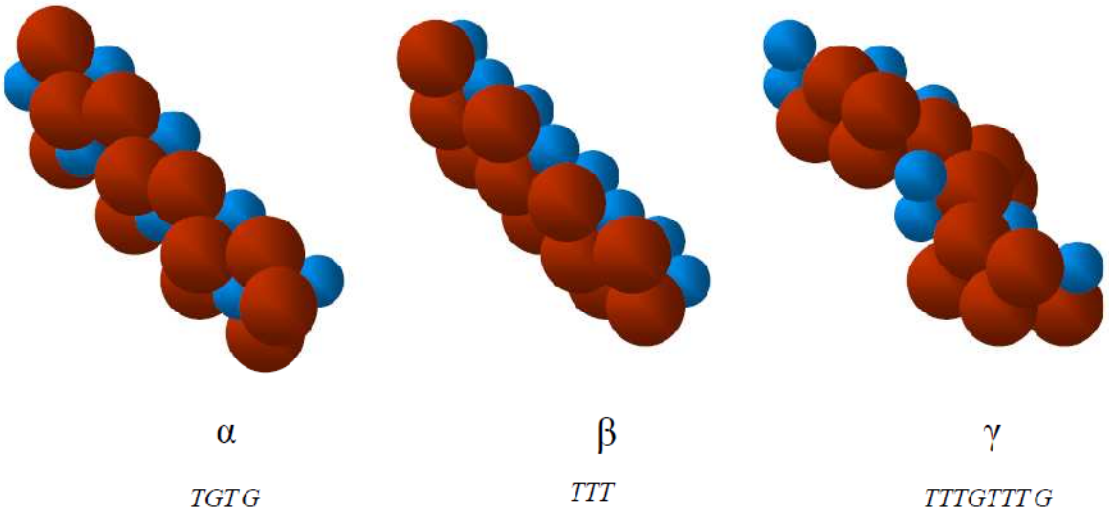

Figure 1.3: Space filling models of PVDF in three conformations.

The figure 1.3 shows the space filling model of PVDF in all the three conformations. As we can see α-phase is more homogenous. This enables it to be stable in nature and is non-polarized because of mixed positive and negative charges. The polymer chains are transferred from α to β-phase when the films are stretched or rolled by deformation at below 100°C, or under continuous high electrical field. The β-phase has a net dipole moment and best piezoelectric coefficient after appropriate poling process. That is the reason there are many extensive works to make β-phase PVDF films.

1.2 Morphology of PVDF

Polymer crystals are extremely small and when grown from the melt, are arranged into essentially spherically symmetric poly-crystalline aggregates that have no net polarization. These aggregates are called spherulites and result from nucleation of primary crystals within the melt, followed by radial growth outward from these nuclei in spherical envelopes.This microstructure appears as radial fibers which are in fact stacks of very thin, platelet-like crystals, called lamellae (about 10 nm thick and several micrometers in lateral dimensions). These lamellae consist of macromolecular segments that are packed crystallo-graphically, while the intervening amorphous regions contain chain segments in disordered

conformations. This two-phase structure of the solid state is typical of crystallizable polymers. In PVDF, crystalline lamellae represent about 50% of the total mass, the other half being amorphous.

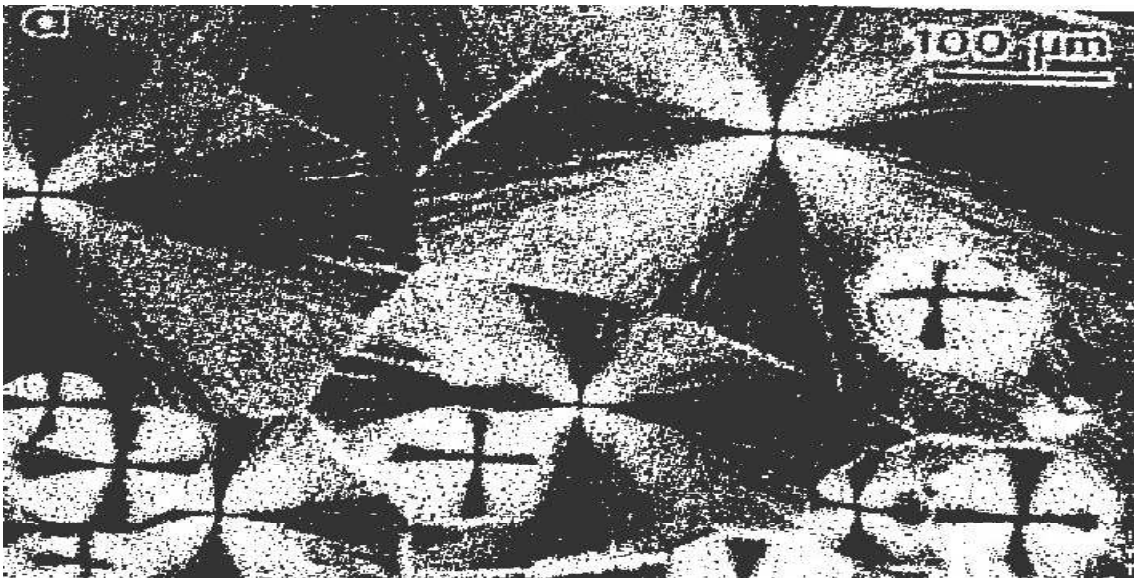

Figure 1.4: Spherulites of PVDF crystallized from crystallized from the melt at 160°C.large spherulites are of the antipolar α-phase; small ones belong to the polar γ-phase**.**

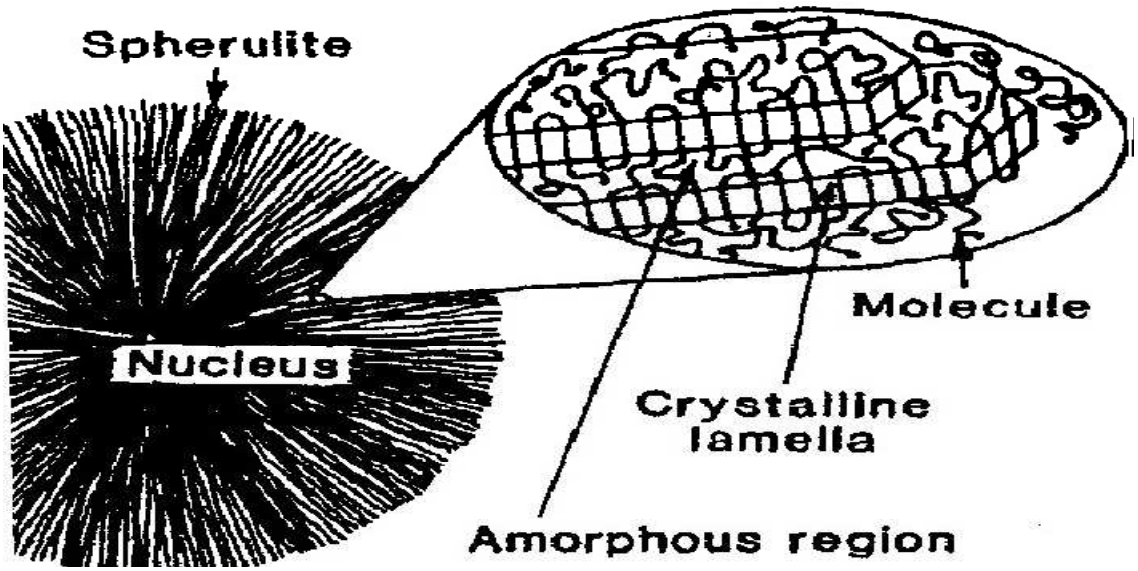

Figure 1.5: Schematic representation of the structure of polymer spherulitic.

1.3 Piezoelectricity, Pyroelectricity and Ferroelectricity in Polymers

The piezoelectric effect was discovered experimentally by the brothers Pierre and Jacques Curie in the year 1880. What the brothers Curie found was that some crystals when

compressed in particular directions show positive and negative charges on certain portions of their surfaces, the charge being proportional to the pressure and disappearing when the pressure is withdrawn. Eventually, the two brothers developed the basics of piezoelectric behaviour and documented responses of materials like Rochelle salt, quartz, and topaz.

During World War I, the piezoelectric quartz plates could be used for detecting submarines. When a voltage is applied to the device, the crystal will expand. Similarly, when a wave strikes the device, it will set the quartz in vibration and generate a voltage which can be detected.

1.3.1 Piezoelectricity

Piezoelectric polymers are subset smart materials. Scientist defines a smart material as "a material that changes one or more of its properties in response to an external stimulus". Piezoelectric materials are a class of materials which can be polarized. Piezoelectricity refers to the generation of an electrical signal in a material in response to a mechanical stress which is known as the direct piezoelectric effect. A linear relationship between mechanical stress and electrical parameters is usually expressed in the following equations:

$$D = d \,.T$$

Where D is electric charge density, T is the applied stress, and d is called piezoelectric stress constant. The resulting electric field E is related to an external stress T through the piezoelectric voltage constant g, which is an important parameter for sensors applications.

The direct effect as shown in figure 1.6 usually the principle of sensors- is defined as when an applied stress to a piezoelectric material produces a charge on the surface.

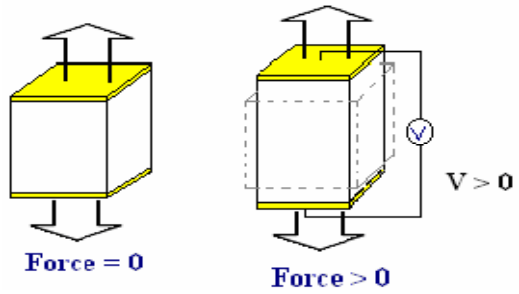

Figure 1.6: Direct piezoelectric effect

The second effect is the indirect or converse effect as shown in figure 1.7 usually the principle of actuators. This happens when the application of a voltage across a piezoelectric material results in a shape change.

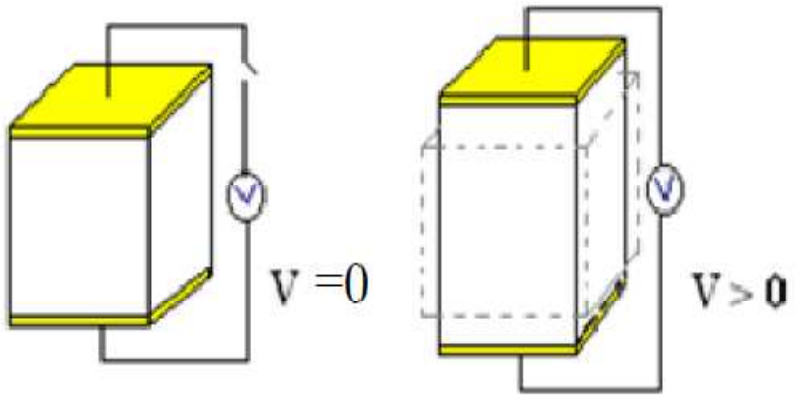

Figure 1.7: Converse piezoelectric effect.

1.3.2 Pyroelectricity

Pyroelectricity refers to the generation of an electric signal in response to a change in temperature. Consequently, the pyroelectric coefficient *p* is defined by equation

$$\Delta P = p\,\Delta T$$

Where ΔP is the reversible change in polarization and ΔT is the change in temperature. The charge to be measured as a result of a temperature change will depend on the surfaces upon which the measuring electrodes are placed. In thin polymer films, the electrodes are almost always placed on the large flat surface, and the net polarization direction is normal to this surface. At equilibrium, the polarization is equal to the charge (Q) per unit area (A). Therefore, the pyroelectric coefficient p is defined as the change in polarization per unit change in temperature; the usual experimental apparatus consists of measuring the charge per unit area generated by a unit change in temperature, which means that the pyroelectric coefficient is given in Equation

$$p = \frac{1}{A}\left(\frac{dQ}{dT}\right)$$

1.3.3 Ferroelectricity

The group of dielectric materials called ferroelectrics exhibits spontaneous polarization in absence of an electric field. There must exist in ferroelectric materials permanent electric dipoles, the origin of which is explained for barium titanate, one of the most common ferroelectrics.

Ferroelectric materials such as barium titanate go through a phase transition from a centrosymmetric non-polar lattice, to a non-centrosymmetric polar lattice at the critical temperature. Also, there is an important characteristic of ferroelectric materials is called a domain as shown in figure 1.8, which is a microscopic region of a crystal in which the polarization is homogenous. These domains are naturally un-aligned, but can be aligned by applying a DC electric field for an extended period of time, which is known as poling. In semicrystalline polymers such as PVDF, there are regions where the chains exhibit amorphous and crystalline regions. Consequently, the crystalline phase must have a net dipole moment that can be oriented by applying an electric field. Dipole alignment occurs by rotation of molecular segments within the crystal about the main chain.

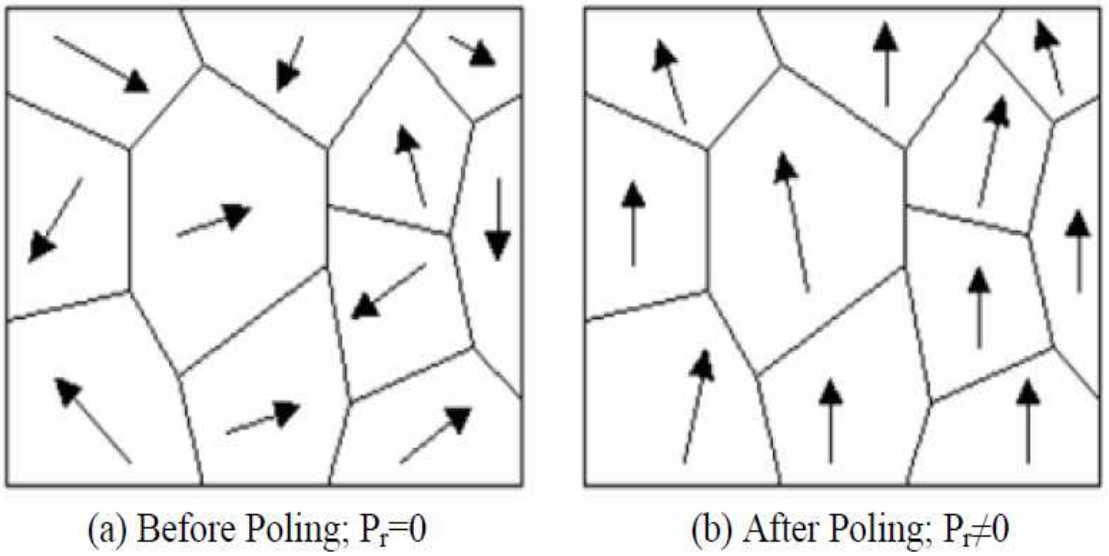

Figure 1.8: A diagram of ferroelectric domain structure (a) before poling, and (b) after poling.

Polyvinylidene fluoride is a ferroelectric polymer. Ferroelectric materials are classified as nonlinear dielectrics. This means that when an electric field (E) is applied to the material, the stored (Q) does not result in a linear response.

1.4 Polymer Crystallization

When a polymer is cooled down from the melt or concentrated from a dilute solution, molecules are attracted to each other forming a solid mass. In doing so, two arrangements are possible: first, molecules vitrify, and the random coil and entanglement are frozen; second, the individual chains are folded and packed in a regular manner characterized by three dimensional long range orders. The concept of crystallinity in polymers must be viewed

slightly different from small molecules. Normally crystalline domains containing many imperfections coexist and are connected with disordered amorphous domains by polymer chains running through. Consequently crystalline polymers are termed as semi-crystalline polymers. Polymer crystallization is a relatively slow process and it occurs over a range of temperature as contrast to small molecules crystallization. The tendency for a polymer to crystallize depends on the magnitude of intermolecular bonding forces as well as structure features such as structure regularity, chain flexibility, polarity and size of substituents.

1.4.1 Lamellar Structure

When polymers crystallize from melt or solution, most of cases, it will form thin lamellae structure as shown in figure 1.9, with a thickness about 100 Å, in which the molecules are folded back and forth on themselves. The size, shape, and regularity of the crystals depend on their growth conditions. Such factors as solvent, temperature, concentration, and rate of growth are important. The thickness of the lamellae, for instance, depends on the crystallization temperature as well as any further annealing treatments. For some polymers, in order to obtain single crystal lamellar it is desirable to have crystallization take place at an elevated temperature, as close to the melting point as possible. At these temperatures the molecules have sufficient mobility to disentangle and pack into lattice. It is thus desirable to use a relatively poor solvent.

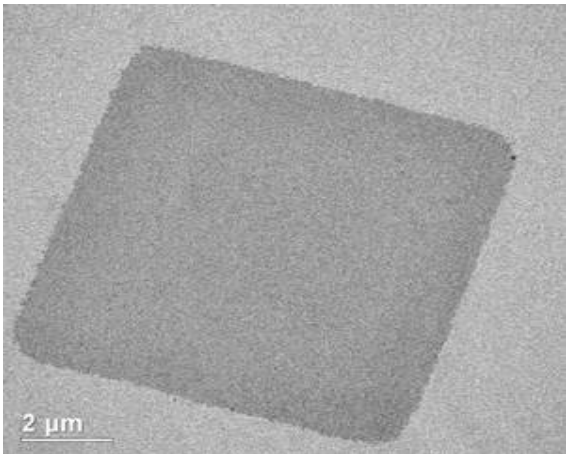

Figure 1.9: Optical light image of a PEO single crystal lamellar

1.4.2 Spherulite Structure

Crystallization of many polymers from melt often results in so called spherulites that are large enough to be observed in optical microscopy. As the name suggested, they are in the

spherical shape. Polymer spherulites are not single crystals, but contain both crystalline and amorphous domains.

One unique feature of polymer spherulites is the so called Maltese cross as shown in figure 1.10. The origin of the pattern is from anisotropic nature of polymer optical properties. There is a difference in the refractive index along polymer chain direction and the perpendicular direction. When a light passes a polarizer and polymer spherulites, it becomes out of plane and thus appears dark after come out from the second polarizer at θ =0° and 90°.

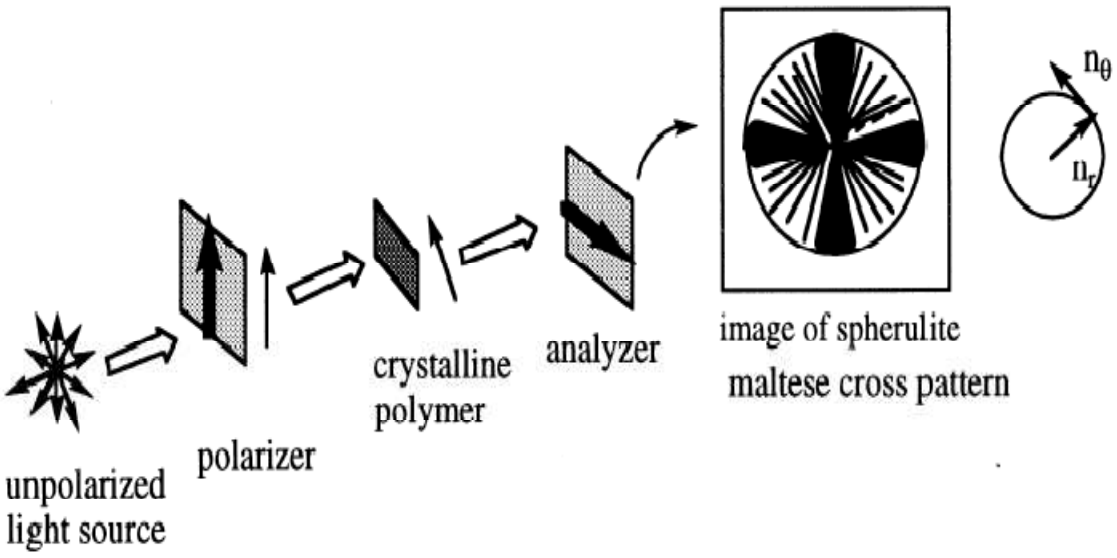

Figure 1.10: Polarized light microscopy (PLM) experimental set up

1.4.3 Shish kebab Structure

Polymer shish kebab crystals were formed under shear field in melt or solution state. It was first observed in 1960s by Pennings **[5].** His electron micrograph in figure 1.11 shown below cleared showed the structure of flow-induced PE shish kebab crystals. A shish-kebab polymer crystal usually consists of a central fibril (shish) and disc-shaped folded-chain lamellae (kebab) oriented perpendicularly to the shish. It is generally understood that the shish of these crystallites was formed by crystallization of fully stretched or extended chains. The kebabs are believed to be folded-chain lamellar structures. The growth direction of the kebabs is normal to the shish. The chain alignment in the kebabs is parallel to the shish.

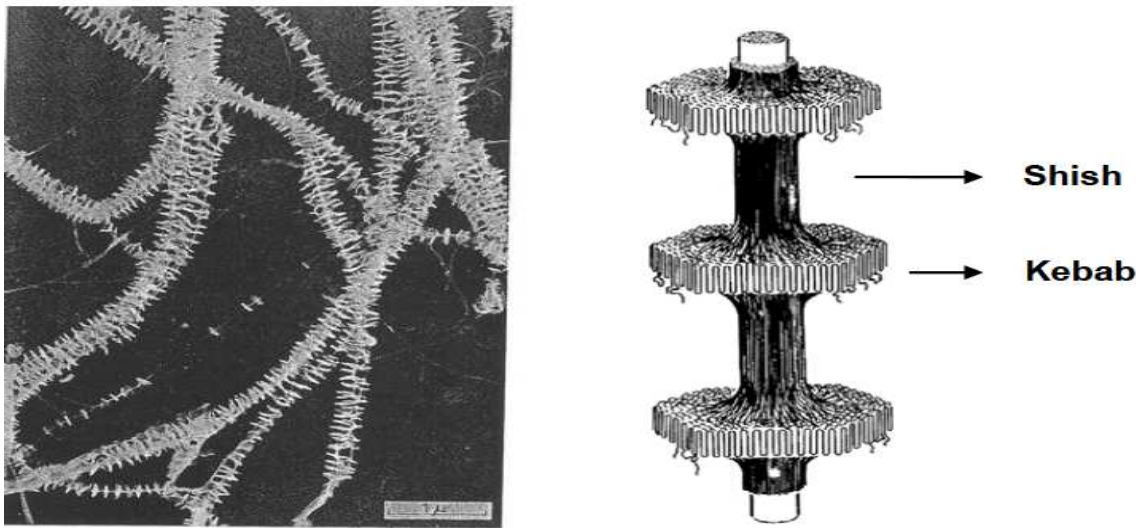

Figure 1.11: Electron micrograph and schematic of shish kebab structure.

1.5 Polarization Process for PVDF

The most common method for obtaining macroscopically polar films in PVDF involves first mechanical extension and then electrical poling as described by the figure 1.12:

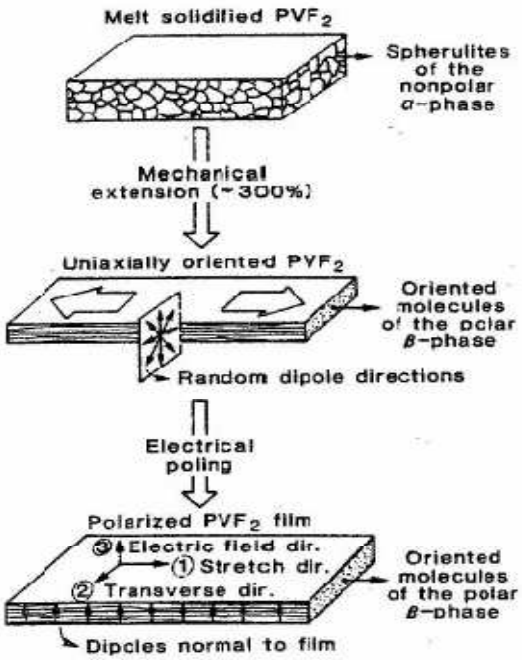

Figure 1.12: Representation of the processes commonly employed to obtain piezoelectrically active PVDF films.

Mechanical drawing causes a breakdown of the original spherulitic structure into an array of crystallites whole molecules are oriented in the direction of the force. At high temperature

(~150°C) deformations, the original TG+TG- chains get free to slide past each other without altering their conformation, so that the resulting structure still remains the α - phase. However, a deformation at low temperatures (~ 90°C) results in a molecularly oriented morphology belonging to β - phase **[6].** However, as seen from the figure 1.12 above, the dipole vectors are still not uniquely oriented but lie randomly in planes normal to the molecular chains. Thus it is required to align these dipoles in the direction of an externally applied field normal to the film.

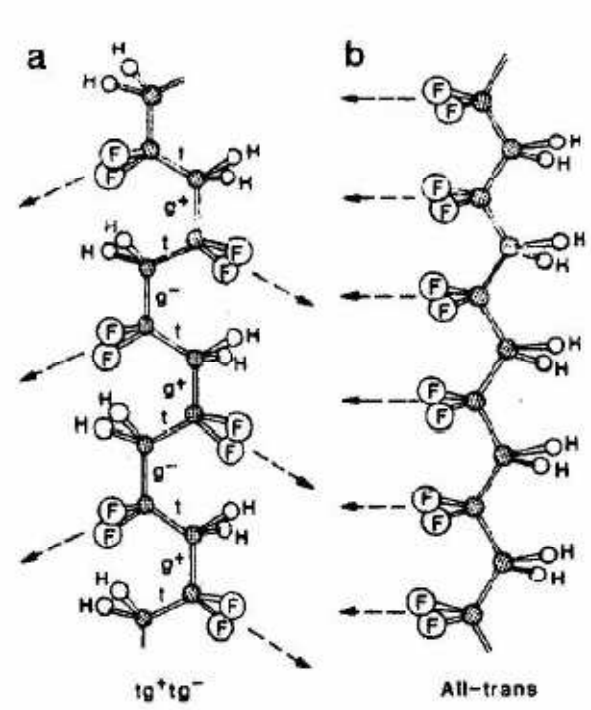

Figure 1.13: Schematic depiction of the two most common chain conformations of PVDF crystals: (a) TG+TG- (b) TTTT. The arrows indicate the projections of the CF_2 dipole moments in the plane containing the carbon backbone.

It has also been shown that the anisotropy disappears at high poling fields, that dipoles are, in fact, reoriented during application of an electric field, and that other typical phenomena accompanying ferroelectricity – hysteresis loops and Curie transitions – are also seen in PVDF **[7].**

A common method of poling is to apply a static electric field on the order of 0.5 MV/cm at approximately 100°C with a low current, high voltage DC power supply for up to one hour; this is called thermal poling as shown in figure 1.14. Commercially available PVDF films, however, are typically poled via corona poling figure B because this technique is amenable to mass production and results in a product with a more stable polarization over time. In this

process, a corona discharge caused by a high electric field, ionizes the air surrounding a grounded sample; these ions deposit and create a potential across the sample resulting in poling.

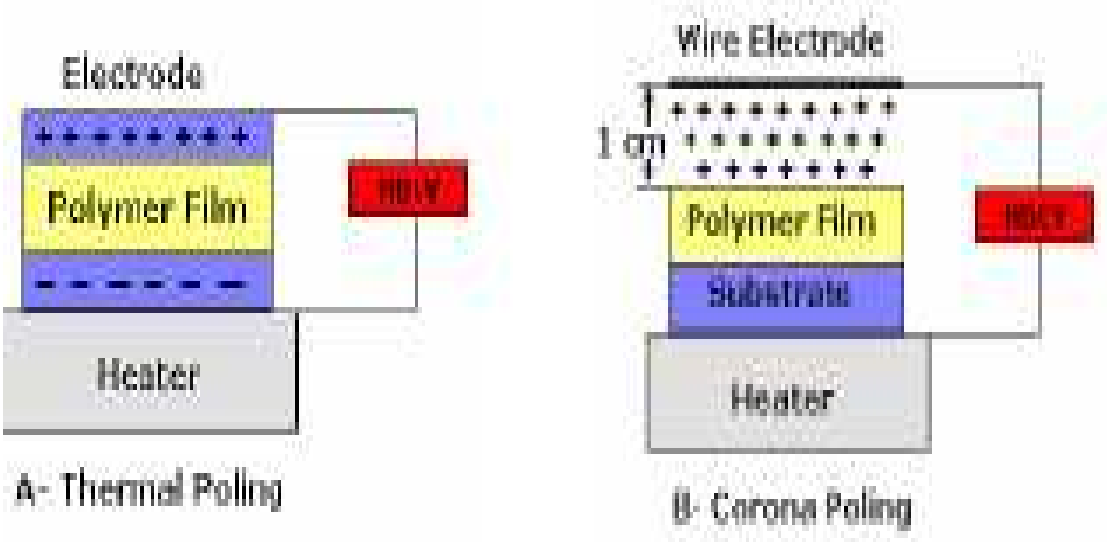

Figure 1.14: Types of polymer poling

1.6 Dielectric and Polarization in Polymers

Polymers are dielectrics, and dielectric materials are insulating materials. The dielectric constant of a material is defined as the ratio of the capacitance of a condenser containing a material to the capacitance of the same condenser without that material (under vacuum) as shown in figure 1.15. The capacitance of a condenser measures the ability of a capacitor to store charges.

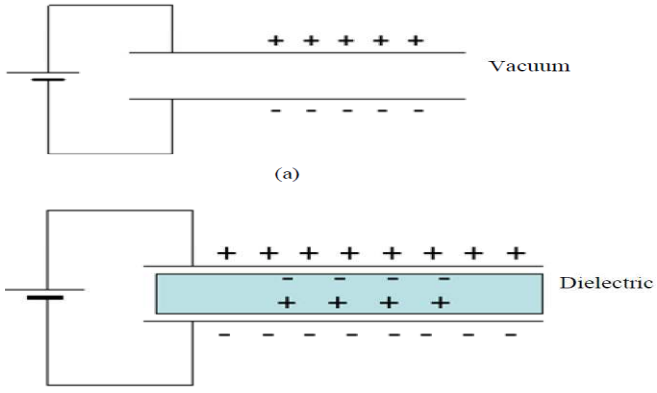

Figure 1.15: (a) Surface charge on a condenser with vacuum, and (b) Surface charge on a condenser with dielectric material.

The dielectric constant of the material depends on the material's polarization; the displacement of the charge by applying the electric field is called "polarization". The higher

the polarizability of the molecules, the higher the dielectric constant. For many dielectric materials, polarization is proportional to electric field through Equation.

$$P - \varepsilon_{\circ}(\varepsilon' - 1).E_p$$

Where *P* is the polarization in C/m^2, ε_0 is permittivity of the vacuum in F/m, ε' is the dielectric constant, and *Ep* is the applied electric field in V/m.

Polarization mechanisms have several types discussed below:

There are four different types of polarization mechanism that can affect the dielectric constant and dielectric loss of the material: electronic polarization, atomic polarization, orientation polarization and interfacial polarization. In a given dielectric material, the total polarization is a sum of all the polarizations resulting from each one of them.

The polarizability of non-polar molecules arises from two polarization mechanisms, electronic and atomic. While in polar molecules depend on dipolar and interfacial polarization mechanisms.

Electronic polarization mechanism occurs at the molecular level and arises from a shift of the center of mass of the negative electron charge cloud surrounding the positive atomic nucleus when an electric field is applied, as shown in figure 1.16. This charge displacement acts to neutralize part of an applied field. This occurs in materials where the structure is formed from the molecules of different atoms with different electro negativities. Forming molecules of different types of atoms, results in the displacement of their electron clouds towards the stronger binding atom. This shift of the electron cloud results in change of atoms polarity, whose equilibrium position is further changed when electric field is applied.

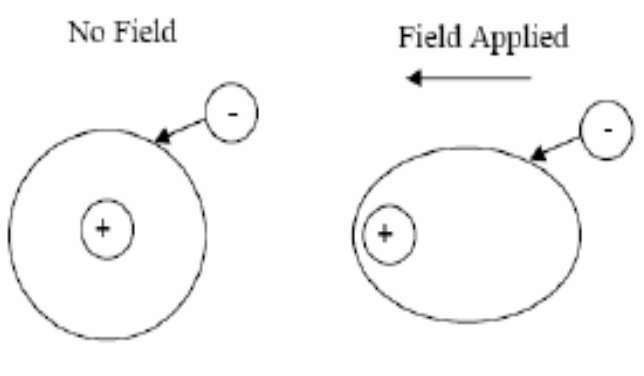

Figure 1.16: Effect of electric field on electronic polarization

Atomic polarization mechanism occurs due to the shift of the atom itself, and it is usually due to the deformation of positive and negative atoms under the force of the applied field. Figure 1.17 is a schematic diagram of the atomic polarization.

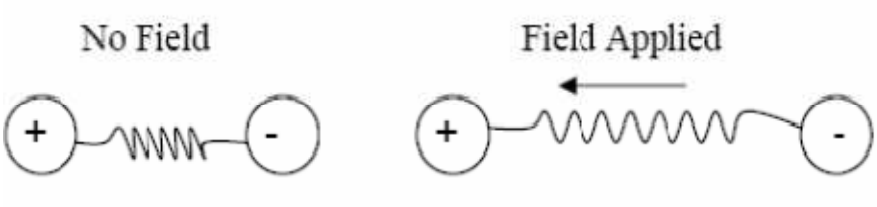

Figure 1.17: Effect of electric field on atomic polarization

Dipolar polarization mechanism, also known as orientation polarization, occurs when applying field to a randomly oriented dipolar material, in which the applied field cause a net orientation parallel to it, as illustrated in figure 1.18.

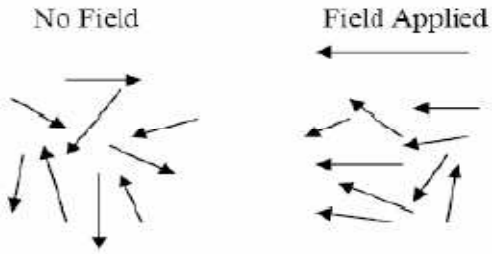

Figure 1.18: Effect of electric field on dipolar polarization

Interfacial polarization, also known as ionic relaxation, is comprised of ionic conductivity and space charge relaxation. Ionic conductivity predominates at low frequencies and introduces only losses to the system. Interfacial relaxation occurs when charge carriers become trapped at interfaces of heterogeneous systems. A schematic of interfacial polarization mechanism is shown in figure1.19.

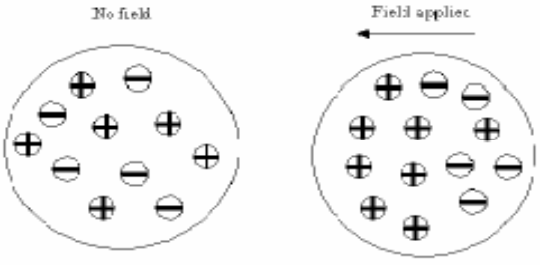

Figure 1.19: Effect of electric field on interfacial polarization

Electronic, atomic, and orientation polarization are all due to the charges that are locally bound in atoms, molecules, or the structures of solids and liquids. In addition to that, charge carriers usually exist that can migrate for some distance through the dielectric material. When the charge carriers are impeded in their motion, either because they become trapped in the material or at an interface or may be because they cannot be freely replaced at the electrodes,

space charge and a macroscopic field distortion result. This kind of distortion appears as an increase in the capacitance of the sample and may be indistinguishable from the real rise of the dielectric constant. Free charge carriers migrating through the crystal under the influence of an applied field may be trapped by a defect for example lattice vacancies, impurity centers, dislocations. The effect of this will be the creation of a localized accumulation of charge that will induce its image charge on an electrode and give rise to dipole moment, which contributes to the interfacial polarization.

It is worthy to mention that dielectric properties highly depend on temperature. Electronic polarization is not dependent on temperature as the shift of mass of the negative electron charge cloud around the nuclei is not affected. Orientation polarization depends on temperature since the ability to align and to rotate a dipole is temperature dependent because the mobility of dipoles is influenced by temperature and also because the thermal fluctuations resist the influence of the field in aligning dipoles. Orientation polarization drops rapidly with further increase in temperature because the increase in temperature reflects increasing the energy associated with the thermal motion (kT), which opposes the alignment of dipoles in the field. Interfacial polarization is temperature dependent because charge mobility is temperature dependent.

Each dielectric mechanism effect has a characteristic relaxation frequency. As the frequency becomes larger, the slower mechanisms drop off. A dielectric permittivity spectrum over a wide range of frequencies includes the real and imaginary parts of permittivity are shown in figure 1.20. Electronic and atomic polarizations due to the inertia of orbiting electrons, known as the inertia effect, have a small magnitude except at the resonant frequency. Electronic polarization occurs at a characteristic frequency of about 10^{15} Hz and atomic polarization occurs at about 10^{12} Hz. Lower frequencies of Each dielectric mechanism effect has a characteristic relaxation frequency. Electronic and atomic polarizations due to the inertia of orbiting electrons, known as the inertia effect, have a small magnitude except at the resonant frequency. Electronic polarization occurs at a characteristic frequency of about 10^{15} Hz and atomic polarization occurs at about 10^{12}Hz.

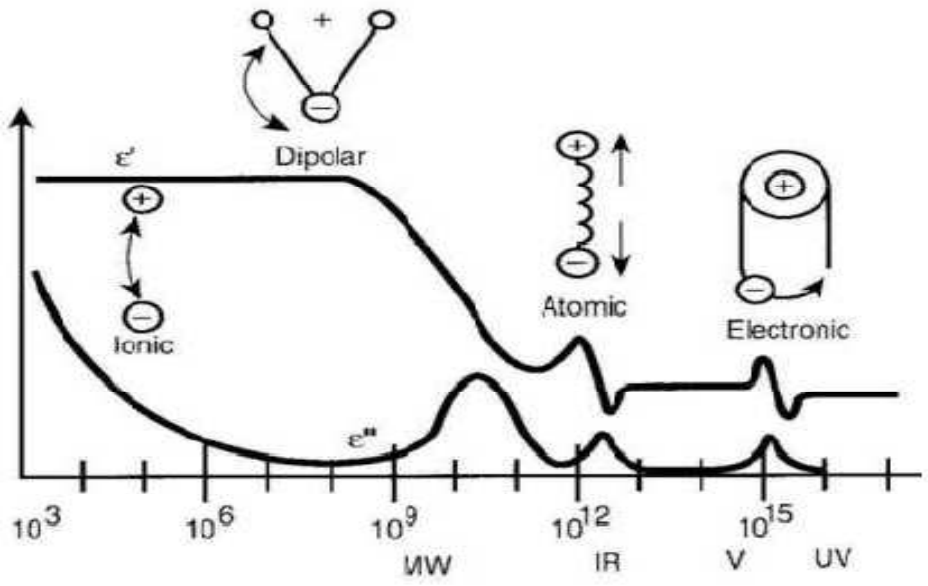

Figure 1.20: Frequency response of the dielectric mechanism.

1.7 Electric conduction mechanism in polymers

Normally, at the low electrical fields, it is found or assumed that the conduction of electrical current in polymers and insulators is ohmic. However, the polymers electrical properties change when subjected to higher electric fields and temperature for long time. The conduction and storage of charge in polymers depends on lot of material parameters such as crystallnity, cross linking and additives **[8].** The electrical conduction mechanism in composites is complicated. The classical conduction and transport mechanisms found in conductors and semiconductors are not found in polymers. This is due to difference in morphology and chemistry of the polymer. Consequently different mechanisms operate. Charge injection from electrodes into polymers, traps and volumetric conduction, tunnelling and hopping conduction were found to play an important role in conduction and charge transport in polymers. Electric conduction may therefore depend on material preparations and their thermal history and it becomes very difficult to determine the conduction mechanism. In general, electric conduction may occur through the movement of either electrons (holes) or ions. The steady state conduction current in composites is controlled by either electrode or bulk processes. Usually, more than one mechanism may operate at the same time, but only one is dominat.

CHAPTER 2
LITERATURE REVIEW

Poly (vinylidene fluoride) (PVDF) is one of the semi- crystalline polymers with at least four crystalline forms referred to as α, β, γ and delta phase, among which the β-phase has gained substantial importance due to its advantageous pyro- and piezo-electric properties **[9]**. It requires a better method to induce the formation of β-phase crystal in order to improve the physical properties of PVDF. β-phase is not usually obtained by crystallization from the melt, but it is normally obtained by various methods including tensile deformation and uniaxial compressional deformation of a phase, quenching and annealing process **[10]**, by applying a strong electric field and crystallizing from solution with appropriate conditions **[11].**

β-phase can also be induced by using different kind of solvents. There is a strong effect of solvent molecules with poly (vinylidene fluoride) (PVDF) chains on the structure and crystallization behaviour of PVDF in films obtained by solution casting. In a single solvent system, the film cast from the good solvent of N,N-dimethylformamide (DMF), showed dominantly β-phase crystals with the highest PVDF crystallnity (50.6%) and the largest spherulite size, about 4 mm, at the top surface. The samples deposited from good swelling agents, such as tetrahydrofuran (THF) and methyl ethyl ketone (MEK), exhibited mainly the original α-phase with some amount of β-phase crystals; the crystallization behaviour and the morphology of the surface were similar to the original PVDF resin, because of the only partially dissolved PVDF chains in these two solvents. In a mixed solvent system (THF/DMF), the β- phase formation with linearly increment in the DMF content resulted in the clear spherulitic structure with higher percentage of β phase. Surface of the film deposited by such mixed solvent systems consisted of β- spherulites with average size of about 3 mm, which were smaller than those grown from pure DMF, because of the increased crystallization rate in the mixed solvent **[12].**

The altering and enhancement of the polymer's properties can tailored through doping with various nano-fillers such as metals, semiconductors, organic and inorganic particles, transition metal halides and fibres, as well as carbon structures and ceramics. Such additives are used in polymers for a variety of reasons such as their extraordinary mechanical, electronic, and optical properties. PVDF and its copolymers have attracted more attentions for their broad applications in piezoelectric ferroelectric and electromechanical applications.

By doping ceramic, semiconductor, metal, metal oxide and carbon nanotubes components, the dielectric constants of the PVDF composites were also enhanced. However the polymer, which was filled with much ceramic, semiconductor, metal, loses its flexibility and limits its use for technological applications.

At the same time the uses of metal salt has been become the important prospective, widely used to increase the β-phase crystallinity of PVDF and consequently enhance the physical properties. The use of metal salt is cost effective method with simple mythology (for solution-cast films) **[3].**

In the past few years some reports have been appeared in the literature, suggesting about induction of β-phase and its application as a composite systems for technogical applications.

In this path way Youn et al. in 2008 presented a report on metal Salt-Induced ferroelectric crystalline Phase in Poly(vinylidene fluoride) films as an effect of varying mass fractions (0–20 wt.-%) of calcium chloride ($CaCl_2$) salt on the α- and β-phase content of (PVDF) as-cast films. Their finding shows that higher percentage of ferroelectric β-phase for 15 wt percent $CaCl_2$ loaded PVDF composite film as compared to neat PVDF **[3].**The filling level (W) dependence of the local structure of $MnCl_2$ through the PVDF matrix was explored by Tawansi et al. in 1998 **[13].** In 1999 Tawansi et al. reported a report on Poly (vinylidene fluoride (PVDF) films, filled with various mass fractions (w = 15%) of $MgCl_2$. The effect of crystalline and electronic structural variations, due to filling level, on the d.c.- electric conduction was investigated **[15].** Consequently Tawansi et al. in 2003 reported the effect of $CuCl_2$ and $CoCl_2$ mixed fillers on the physical properties of PVDF films. Their results suggesting that the crystallinity of PVDF phase's increases as the concentration of filler increased **[16].** With the continuous growth of the field Abdelaziz et al. presented a report discussing about the effect of equal amounts of Mn and Co on the microstructure and physical properties on the PVDF films **[17].** Ferroelectric properties of PVDF such as ferroelectric polarization switching, phase transition studies also be studied with different nitrate salts such as KNO_3, $NaNO_3$, $CsNO_3$ **[18-20].** Poly (vinylidene fluoride) (PVDF) films filled with mixed fillers of $CuCl_2$–$MnCl_2$ were reported by Abdelaziz et al. in 2004 **[21].** Poly (vinylidene fluoride) (PVDF) film filled with calcium carbonate ($CaCO_3$) were also introduced to the field **[22].** The effect of alkali metal salts on the structure and morphology of PVDF films also investigated by Wang et al. in 2009 **[23-24].**

2.1 GAP IN STUDY

Poly (vinylidene fluoride), is a polymer that has been studied for over four decades due to its stability and durability in various environments. PVDF Poly (vinylidene fluoride) is main material of interest due to its piezo and ferroelectric properties. The extensive literature review gives an idea that the physical properties of polymer can be enhanced by mean of adding nanoparticles, carbon nanotubes and metal salts where the concentration can be varied and optimize to understand the physical structural and chemical properties of the composite system. The relationships between structure and physical properties of PVDF/MWCNT have been discussed earlier and well documented in the literature facilitate various applications in diverse fields. The use of metal salt in PVDF as dispersed medium in the mixed solvent system can be used to increase the crystallinity of PVDF (for longer retention time and fatigue characteristics) and surface morphology (to reduce electrical shortage). Such transitions metal salt (TMS) filler can be loaded in the PVDF matrix up to higher concentrations, which can enhance the physical properties of composite systems. This can serve as predominant candidates for electronic applications and will also be the scope of future research.

2.2 AIM OF WORK AND OBJECTIVE

The main objective of our study is to produce and investigate metal salt dispersed PVDF composites. The study will be focused on the examination of the structural and physical thermal and electrical properties of polymer composites.

The main objectives of study are:

1) Synthesis of metal salt dispersed PVDF β-phase in mixed solvent system.
2) Structural, morphological, chemical and thermal analysis of metal salt dispersed PVDF composite
3) Investigation on electrical properties of metal salt modified composite system.

CHAPTER 3
EXPERIMENTAL

3.1 Materials

The materials used in this study were poly (vinylidene) fluoride PVDF (pellet) having typical M_w=530.000 (Aldrich), Zinc Chloride (Dry) M_w=136.29 (Lobachemie), Cupric Chloride (Dihydrate) $CuCl_2.2H_2O$ M_w=170.48 (Lobachemie), Nickel Chloride extra pure (Hexahydrate) $NiCl_2.6H_2O$ M_w=237.69 (Lobachemie). The solvents used during synthesis tetrahydrofurane (THF), C_4H_8O (M_w=72.11 stablized) (S.D.fine-chem Ltd), N,N-Dimethylformamide DMF, C_3H_7NO (M_w=73.09) (S.D.fine-chem Ltd) and N,N-Dimethylacetamide DMA, C_4H_9NO (M_w=87.12) (Lobachemie). All the materials were used as received without any further purification.

3.2 Synthesis of β-phase Poly (vinylidene fluoride) (PVDF)

The glass wares (three necks round bottom flask, measuring cylinder, and beaker) were first cleaned and rinsed with distilled water and then dried in vacuum oven. All the materials and solvents are weighed with help of electronic weighing balance and mixed in cleaned round bottom flask. A 100 ml three neck flasks is charged with poly (vinylidene fluoride) dissolved in THF/DMF mixture with 5:5 mass ratio. The reactants were refluxed at 60^oC with gentle stirring for 3h on hot plate.

Figure 3.1: Experimental set up for the sample preparation

After stirring for 3h, reaction mixture is allowed to cool to room temperature. The transparent solution is cast on glass substrates by spin coating and rest of the solution poured into beaker

to prepare bulk film. The residue of THF and DMF was allowed to evaporate in air for about one week at room temperature. Free standing thin films (thickness ~ 5-7 μm) on glass substrate were formed at the end with the complete evaporation of solvents.

3.2.1 Chemical composition

Table 3.2.1 THF: DMF (5:5)

Sr.No.	Chemical name	Chemical formula	Quantity of Material used
1.	Poly(vinylidene fluoride) (PVDF)	-(CH_2-CF_2)-	1g
2.	Tetrahydrofurane (THF)	C_4H_8O	5ml
3.	N, N-Dimethylformamide (DMF)	C_3H_7NO	5ml

3.2.2 Spin coating

Spin coating is the preferred method for deposition of thin and uniform films on flat substrates. In the typical procedure the appropriate amount of polymer solution is poured in the center of the substrate.

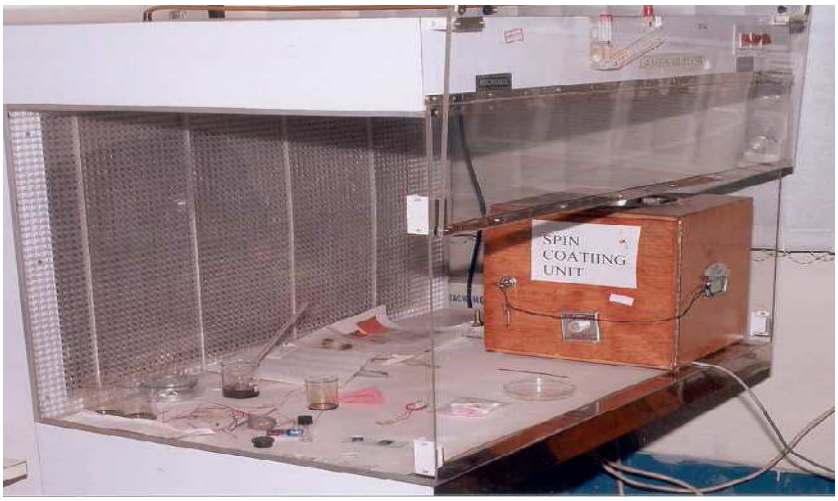

Figure 3.2: Spin coating unit for depositing thin PVDF composite films

The substrate is then rotated at high speed in order to spread the fluid by centrifugal force. Rotation is continued for some time, with fluid being spun off the edges of the substrate, until

the desired film thickness is achieved. The solvent is usually volatile, providing for its simultaneous evaporation with the passage of time.

3.2.3 Cell preparation for dielectric studies

Dielectric measurement of thin film samples are carried out by depositing thin film on ITO coated glass substrate by spin coating unit then sandwiched by another ITO coated glass plate followed by sealing and electrical connection with indium. The detailed description of cell preparation shown in the figure 3.3.

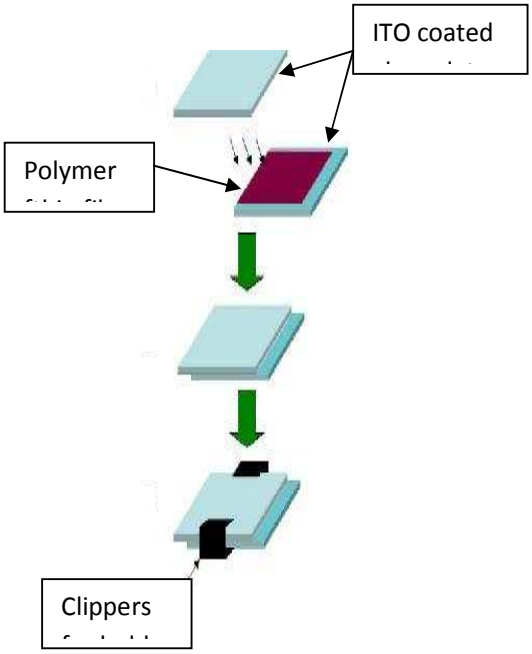

Figure 3.3: Schematic of sample preparation for dielectric studies.

3.3 Polymer-Composite preparation

In order to prepare composite system the first step is same as the synthesis of PVDF samples. In second step, an appropriate amount of metal salt $CuCl_2$ is added to mixture of poly(vinylidene) fluoride and organic solvent N,N-dimethylformamide (DMF) and tetrahydrofuran (THF). After refluxing the mixture at 60^oC for 3 h the appropriate amount of metal salt was dispersed in the system. Then the solution was set for sonication for 1 h. The final mixture was further treated for making of thin film and bulk films by using various techniques i.e. Spin Coating and Solution Cast Method.

The residue of DMF and THF is allowed to evaporate in air for about a week at room temperature. Free standing thin films (thickness ~ 5-7 μm) on glass substrate and bulk film (thickness~ 1-1.5 mm) were formed at the end when the solvent was completely evaporated. The same procedure was followed for rest of the two salts $NiCl_2$ and $ZnCl_2$.

3.3.1 Chemical Composition

Table 3.3.1: Material taken for PVDF-$CuCl_2$ composite (0.5wt%, 1wt%, 3wt%, 5wt%, 10wt%, 15wt%, 25wt %).

Sr.No.	Chemical name	Chemical formula	Quantity of Material used
1.	Poly(vinylidene fluoride) (PVDF)	-(CH_2-CF_2)-	1g
2.	Cupric Chloride	$CuCl_2$	0.5, 1, 3, 5, 10, 15, 25 wt%
3.	Tetrahydrofurane (THF)	C_4H_80	5ml
4.	N, N-Dimethylformamide (DMF)	C_3H_7NO	5ml

Table 3.3.2: Material taken for PVDF-$NiCl_2$ composite (0.5wt%, 1wt%, 3wt%, 5wt%, 10wt%, 15wt%, 25wt %).

Sr.No.	Chemical name	Chemical formula	Quantity of Material used
1.	Poly(vinylidene fluoride) (PVDF)	-(CH_2-CF_2)-	1g
2.	Nickel Chloride	$NiCl_2$	0.5, 1, 3, 5, 10, 15, 25 wt%
3.	Tetrahydrofurane (THF)	C_4H_80	5ml
4.	N, N-Dimethylformamide (DMF)	C_3H_7NO	5ml

Table 3.3.3: Material taken for PVDF-$ZnCl_2$ composite (0.5wt%, 1wt%, 3wt%, 5wt%, 10wt%, 15wt%, 25wt %).

Sr.No.	Chemical name	Chemical formula	Quantity of Material used
1.	Poly(vinylidene fluoride) (PVDF)	-(CH_2-CF_2)-	1g
2.	Zinc Chloride	$ZnCl_2$	0.5, 1, 3, 5, 10, 15, 25 wt%
3.	Tetrahydrofurane (THF)	C_4H_80	5ml
4.	N, N-Dimethylformamide (DMF)	C_3H_7NO	5ml

3.4 Synthesis of β-phase using THF/DMA

We also synthesized the β-phase using another solvent N, N-Dimethylacetamide (DMA) in the mixed solvent system. For this we choose the four concentrations of THF/DMA as 9:1, 8:2, 7:3 and 5:5. The procedure was same as in the case of THF/DMF.

3.4.1 Chemical composition

Table 3.4.1: Sample 1 THF/DMA (9:1)

Sr.No.	Chemical name	Chemical formula	Quantity of Material used
1.	Poly(vinylidene fluoride) (PVDF)	-(CH_2-CF_2)-	1g
2.	Tetrahydrofurane (THF)	C_4H_80	9ml
3.	N, N-Dimethylacetamide (DMA)	C_4H_9NO	1ml

Table 3.4.2: Sample 2 THF/DMA (8:2)

Sr.No.	Chemical name	Chemical formula	Materiel taken
1.	Poly(vinylidene fluoride) (PVDF)	-(CH_2-CF_2)-	1g

2.	Tetrahydrofurane (THF)	C_4H_80	8ml
3.	N, N-Dimethylacetamide (DMA)	C_4H_9NO	2ml

Table 3.4.3: Sample 3 THF:DMA (7:3)

Sr.No.	Chemical name	Chemical formula	Materiel taken
1.	Poly(vinylidene fluoride) (PVDF)	-(CH_2-CF_2)-	1g
2.	Tetrahydrofurane (THF)	C_4H_80	7ml
3.	N, N-Dimethylacetamide (DMA)	C_4H_9NO	3ml

Table 3.4.4: Sample 4 THF:DMA (5:5)

Sr.No.	Chemical name	Chemical formula	Materiel taken
1.	Poly(vinylidene fluoride) (PVDF)	-(CH_2-CF_2)-	1g
2.	Tetrahydrofurane (THF)	C_4H_80	5ml
3.	N, N-Dimethylacetamide (DMA)	C_4H_9NO	5ml

A flow chart for the experimental work which is followed for the preparation of samples is shown.

FLOW CHART

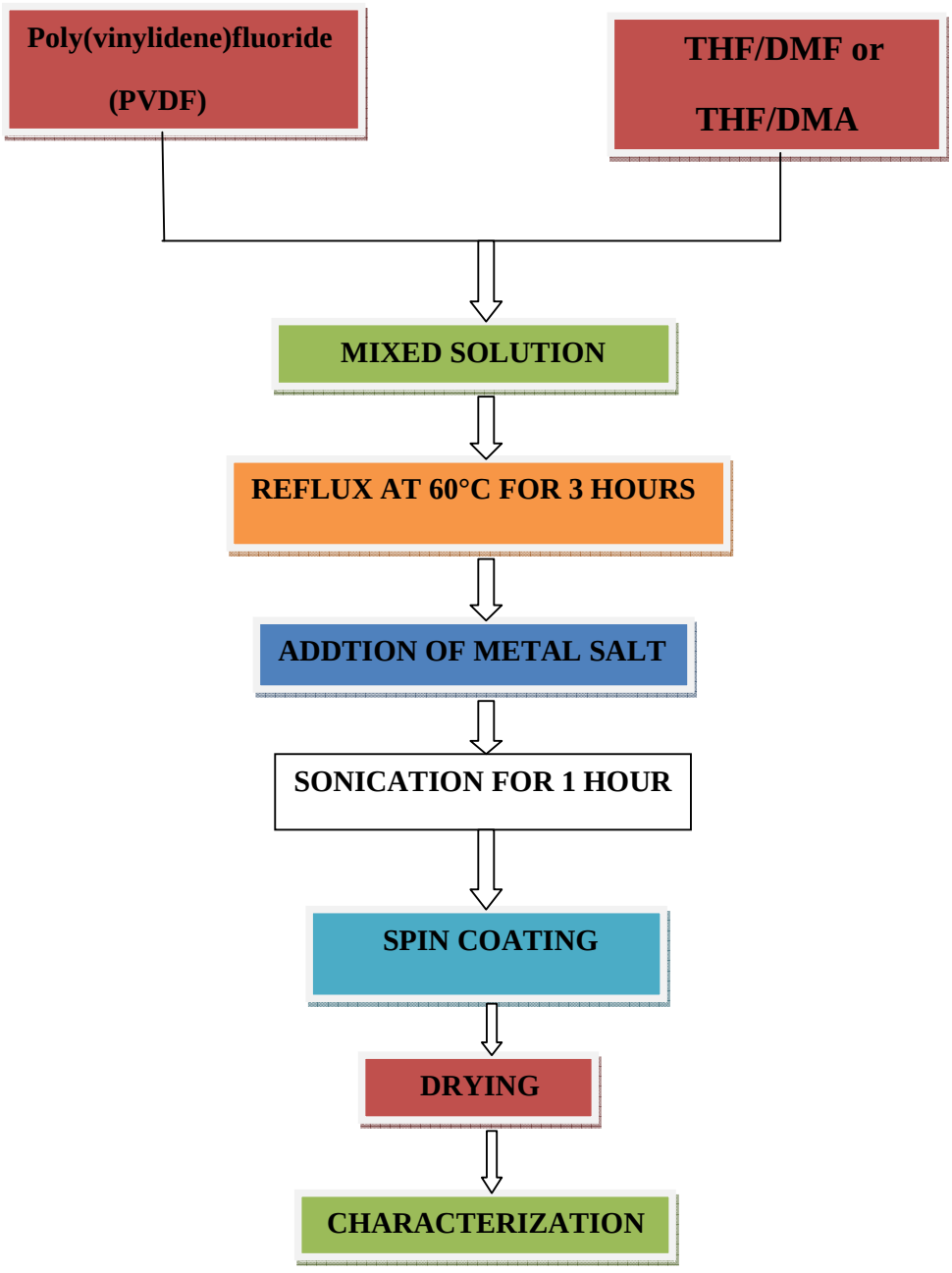

3.5 Characterization techniques

The structural, morphological, chemical analysis, physical, thermal and dielectric measurements of the PVDF films characterized by using various experimental techniques including Olympus optical polarizing microscope, Fourier transformation IR Spectroscopy, X-ray diffraction (XRD), Scanning Electron Microscope (SEM), differential scanning calorimetery (DSC), LCR meter (frequency range 50Hz to 1MHz). The general description of the experimental setups used in this study, as well as conditions and parameters of each experiment are the purpose of the following section.

3.5.1 Fourier transformation IR spectroscopy

FT-IR stands for Fourier Transform Infrared, the preferred method of infrared spectroscopy. FTIR is an analytical technique used to identify organic (in some cases inorganic) materials. This technique measures the absorption of infrared radiation by the sample material versus wavelength. The infrared absorption bands identify molecular components and structures. IR radiation is passed through a sample. Some of the infrared radiation is absorbed by the sample and some of it is passed through (transmitted). When a material is irradiated with infrared radiations, absorbed IR radiation usually excites molecules into a higher vibrational state. The wavelength light absorbed by a particular molecule is a function of the energy difference between the at-rest and excited vibrational states. The wavelengths that are absorbed by the sample are characteristic of its molecular structure. This makes infrared spectroscopy useful for several types of analysis

Figure 3.4: Fourier transforms infrared spectrometer (FTIR)

Typical applications

- Identification of foreign materials
- Particulates
- Fibers
- Residues
- Identification of bulk material compounds
- Identification of constituents in multilayered materials
- It can determine the amount of components in a mixture

3.5.2 X-Ray Diffraction

An x-ray diffraction technique is a non-destructive analytical technique, which reveal information about the crystallographic structure, chemical composition, and physical properties of materials and thin films. These techniques are based on observing the scattered intensity of an X-ray beam hitting a sample as a function of incident and scattered angle, polarization, and wavelength or energy.

Figure 3.5: X- ray Diffractometer

X-ray diffraction (Panalytical X'Pert) is an experimental technique that exploits the fact that x-rays are diffracted by crystals. X-rays have the proper wavelength (in the Angstrom range,

~ 10^{-8} cm) to be scattered by the electron cloud of an atom of comparable size. Based on the diffraction pattern obtained from X-ray scattering of the periodic assembly of molecules or atoms in the crystal, the density can be reconstructed. Additional phase information must be extracted either from the diffraction data.

3.5.3 Wide angle X-ray diffraction

Wide angle X-ray diffraction (WAXD) is an X-ray diffraction technique that is often used to determine the crystalline structure of polymers. This technique specifically refers to the analysis of Bragg Peaks scattered to wide angles, which (by Bragg's law) implies that they are caused by sub-nanometer sized structures.

Wide angle x-ray scattering is the same technique as Small-Angle X-ray Scattering (SAXS) only the distance from sample to the detector is shorter and thus diffraction maxima at larger angles are observed. The diffraction pattern generated allows determining the chemical composition or phase composition of the film, the texture of the film (preferred alignment of crystallites), the crystallite size and presence of film stress. According to this method the sample is scanned in a wide angle X-ray goniometer, and the scattering intensity is plotted as a function of the 2θ angle. When X-rays are directed in solids they will scatter in predictable patterns based upon the internal structure of the solid. A crystalline solid consists of regularly spaced atoms (electrons) that can be described by imaginary planes. The distance between these planes is called the d-spacing. The intensity of the d-space pattern is directly proportional to the number of electrons (atoms) that are found in the imaginary planes. Every crystalline solid will have a unique pattern of d-spacing (known as the powder pattern).

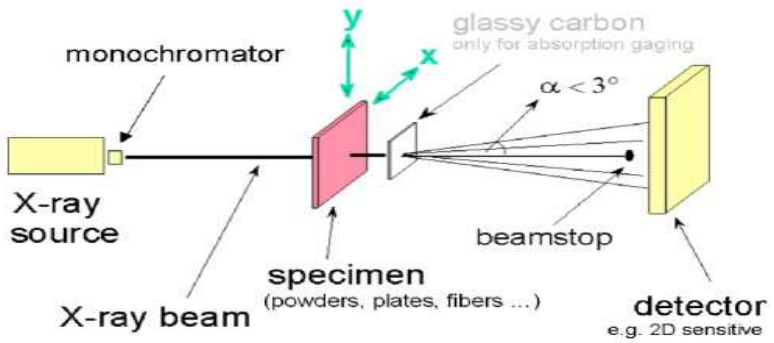

Figure 3.6: wide angle x-ray diffraction

3.5.4 Optical polarizing microscopy

The optical studies observed in pure PVDF, and metal salt dispersed PVDF systems investigated using an Olympus optical polarizing microscope at a magnification of 10X under crossed polarizer using long working distance objective lens. A block diagram of experimental set-up for the investigation of optical textures, dielectric studies and other parameters are shown in figure 3.7.

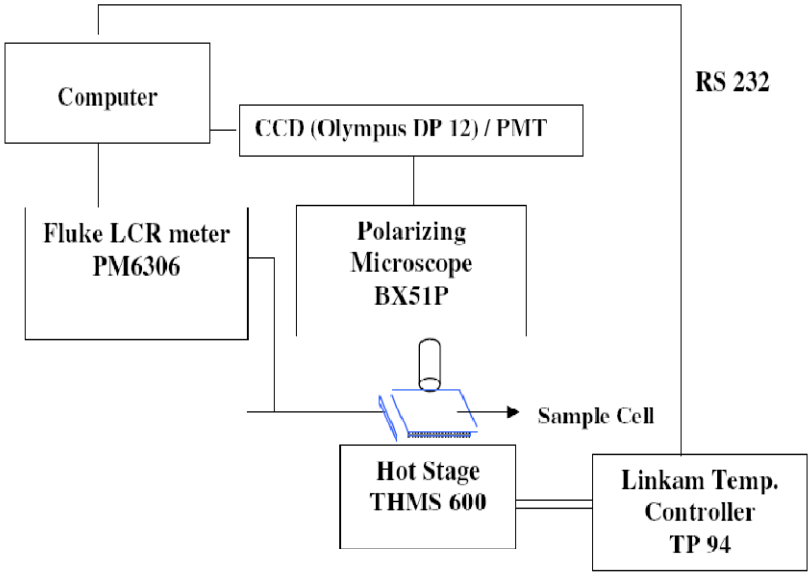

Figure 3.7: Block diagram of the experimental set-up to study the morphological behavior.

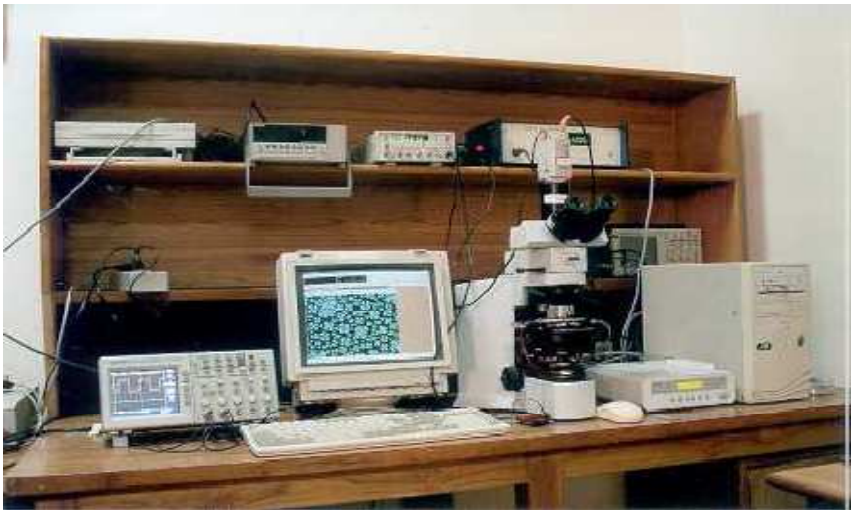

Figure 3.8: Optical Microscope and temperature controller

In dielectric studies, we used Linkam temperature programmer TP94 and ht stage THMS 600. The TP94 is specifically designed for precise temperature control of the Linkam heating/freezing stages. The stage sensor is digitally linearized to give accurate temperature readout, the controls and their functions have been carefully chosen for simple and easy operation. The temperature range is -196°c to 600°c. Heating or cooling rates can be changed almost instantly using the three rate keys. The heat ranges are from 0.1 to 0.9°c/min at 0.1 degree intervals from 1.0 to 9.0°c/min at 1.0 degree intervals.

3.5.5 Differential Scanning Calorimetry

Differential Scanning Calorimetry (DSC) (LINSIS L-63) is a thermal analysis technique used to study the thermal transitions in polymers, such as the melting point temperature, T_m, and the glass transition temperature, T_g. Two pans sit on a pair of identically positioned platforms connected to a furnace by a common heat flow path. The polymer sample is placed in one pan while the other is used as the reference pan. The two pans are then heated or cooled until they reach the selected starting temperature. A typical temperature program is set to increase the temperature at a fixed rate. As the program runs, the system monitors the temperature of each pan and keeps the heating rate constant throughout the experiment. It is important for the system to keep the two separate pans heated at the same rate. The pan with the polymer sample will take in more heat to keep the temperature of the sample pan increasing at the same rate as the reference pan. If the temperature differs from the programmed temperature in either pan, the pan is heated or cooled to keep a constant temperature. The difference in the energy supplied to the two pans per unit time (dq/dt) is proportional to the heat capacity of the sample.

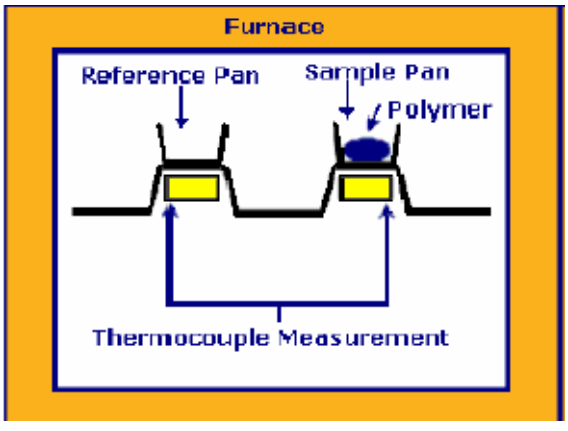

Figure 3.9: Block diagram of Differential Scanning Calorimeter

3.5.6 Scanning electron microscope

The scanning electron microscope (SEM) is a type of electron microscope that images the sample surface by scanning it with a high-energy beam of electrons in a raster scan pattern. The electrons interact with the atoms that make up the sample producing signals that contain information about the sample's surface topography, composition and other properties such as electrical conductivity.

Figure 3.10: Scanning electron microscope

The types of signals produced by an SEM include secondary electrons; back scattered electrons (BSE), characteristic x-rays, light (cathodoluminescence), specimen current and transmitted electrons. These types of signal all require specialized detectors that are not usually all present on a single machine. The signals result from interactions of the electron beam with atoms at or near the surface of the sample. In the most common or standard detection mode, secondary electron imaging or SEI, the SEM can produce very high-resolution images of a sample surface, revealing details about 1 to 5 nm in size. Due to the way these images are created, SEM micrographs have a very large depth of field yielding a characteristic three-dimensional appearance useful for understanding the surface structure of a sample. A wide range of magnifications is possible, from about X 25 (about equivalent to that of a powerful hand-lens) to about X 250,000, about 250 times the magnification limit of the best light microscopes.

The block diagram of SEM set up is shown in the figure 3.11.

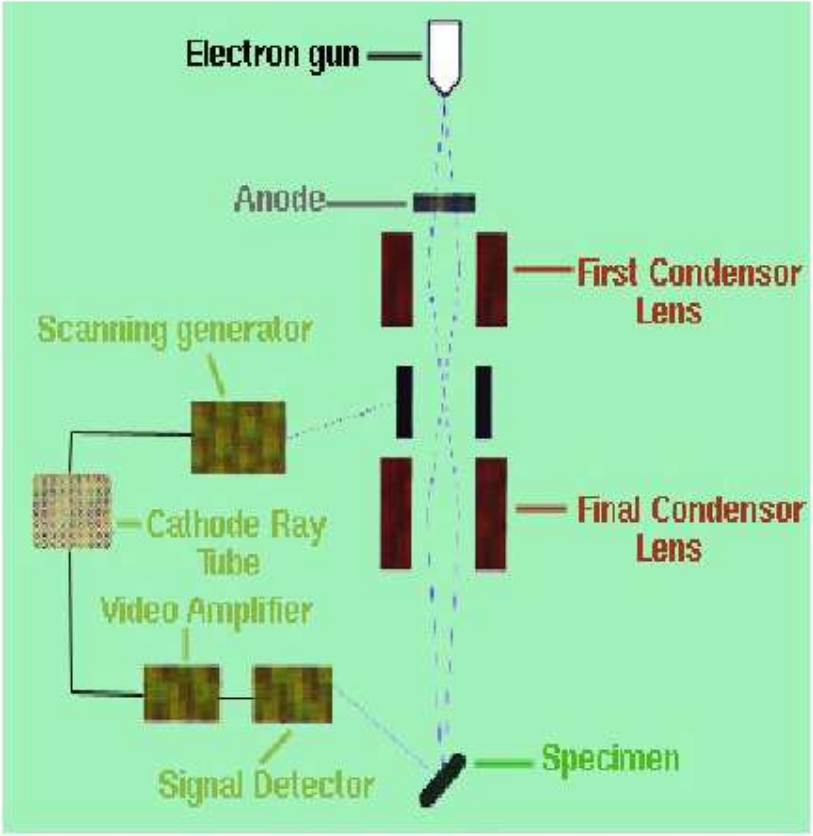

Figure 3.11: SEM Setup

Magnification in a SEM can be controlled over a range of up to 6 orders of magnitude from about X 25 to X 250,000 Unlike optical and transmission electron microscopes; image magnification in the SEM is not a function of the power of the objective lens. SEMs may have condenser and objective lenses, but their function is to focus the beam to a spot, and not to image the specimen. Provided the electron gun can generate a beam with sufficiently small diameter, and SEM could in principle work entirely without condenser or objective lenses, although it might not be very versatile or achieve very high resolution.

3.5.7 Dielectric measurements

The dielectric measurements were carried out using a programmable automatic RCL meter (FLUKE PM 6306) in the frequency range 50Hz to 1MHz. The cell was calibrated using air and benzene as standard references. The frequency and bias dependence of the real and imaginary parts of the complex dielectric permittivity have been studied in detailed at different temperatures. The dielectric properties of the PVDF/Transition metal salts were taken at off voltages.

Figure 3.12: LCR Meter

Dielectric spectroscopy technique measures the dielectric properties of a medium as a function of frequency. In the case of polymeric medium, dielectric spectroscopy is a powerful technique that is capable of probing the molecular motion and the electric properties. The dielectric constant or relative permittivity of a material is the ratio of the dielectric constant of the material to that of vacuum. The capacitance measures the extent to which charge can be stored.

$$\varepsilon_r = \frac{\varepsilon'}{\varepsilon_0}$$

The complex dielectric properties, the relative permittivity (ε') and the loss factor (ε") are determined by scans as a function of frequency and temperature. The displacement of the charge by applying the electric field is called "polarization". The dielectric properties of a material are defined by a complex dielectric permittivity, ε^*

$$\varepsilon^* = \varepsilon' + i\varepsilon''$$

Where ε' is the dielectric constant of the material, also known as the relative dielectric permittivity, and it is used to define the ability of the material to store electrical charge. ε" is the imaginary part, which is related to the material loss and known as the dielectric loss.

Chapter 4
Results and Discussion

This chapter summarise the chemical, structural, morphological, electrical, thermal and dielectric, investigations, with the scope of understanding how mixed and pure solvent affect the formation of crystalline phase of PVDF in the vicinity of TMS. The preliminary confirmation of crystalline phase has been done with Fourier transform infrared spectroscopy (FTIR). While further structure evaluated with X-Ray diffraction analysis. The calorimetric transitions were carried out to understand the variation of thermodynamical variable in these systems and their effect on the physical properties. Dielectric and electrical properties of these systems were performed to identify how the metal salts tailor the physical properties which may produce better prospective for technological applications. The SEM observation gives an idea about the surface morphology, density and porosity of the metal salt dispersed PVDF films which may play vital role to enhance the physical properties. Finally we summarise at the end, the main conclusions obtained from these observations.

4.1. Chemical analysis

To identify the crystalline phase of pure PVDF and $CuCl_2$, $NiCl_2$, $ZnCl_2$ dispersed composite films were scanned with IR spectrometer in the range 400 cm^{-1} to 4000 $cm.^{-1}$. Figure 4.1 (a) displayed FTIR spectrum of the pure (5:5) THF: DMF and $CuCl_2$ (x=0.5, 1, 3, 5, 10, 15, and 25 wt %) dispersed composite films derived from mixed solvent system.

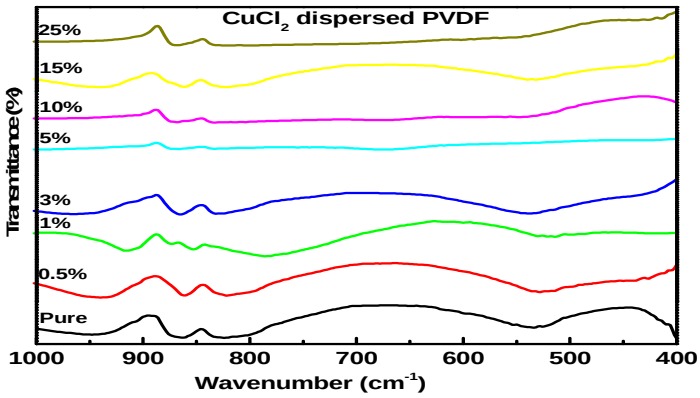

Figure 4.1 (a): FTIR spectra of PVDF-$CuCl_2$ dispersed composite films at different concentrations(x=0.5, 1, 3, 5, 10, 15, and 25 wt %) casted from the mixed solvent solution (5:5 THF/DMF).

The peaks at 510 cm.$^{-1}$ and 845 cm.$^{-1}$, belonging to the β-phase having all-trans (TTTT) molecular conformation (a planar zigzag structure) are assigned to CF bending and wagging modes. With the addition of the varying amount of transition metal salt $CuCl_2$ in the PVDF, the characteristic peaks of α-phase distinctly weakened, and the intensity of β-phase related bands increased significantly up to 3wt%. Though, at higher TMS concentration the β-phase content decreased. Nevertheless, it is clear that the addition of metal salt may have invariably promoted the nucleation of β-phase in PVDF up to a critical filling level, though the reasons behind the reduced rate with further addition of metal salt may attributed to the higher density of metal salt which hinder the nucleation of crystalline phase.

In the similar way FTIR spectrums of $NiCl_2$-PVDF composite films are presented in the figure 4.1 (b).

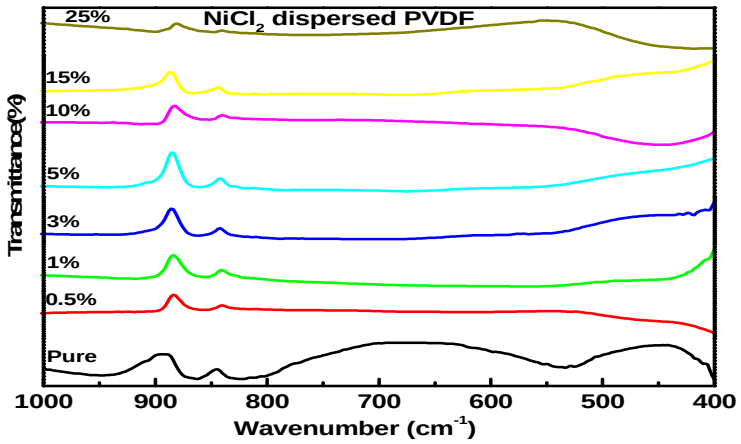

Figure 4.1 (b): FTIR spectra of PVDF-$NiCl_2$ composite films at different concentrations (x=0.5, 1, 3, 5, 10, 15, and 25 wt %) casted from the mixed solvent solution (5:5 THF/DMF).

It was noticed that the peaks appeared at 845 cm^{-1} corresponds to the β-phase of the $NiCl_2$ dispersed composite films, exhibiting the same trend as $CuCl_2$ dispersed system (small decrement in the β-phase content at higher metal salt concentration).

Figure 4.1 (c) shows the FTIR spectrum of $ZnCl_2$ dispersed PVDF films. We observed that small reflection at 510 c.m.$^{-1}$ and stretch at 840c.m.$^{-1}$ inferring about the formation of β-phase. This system also following the same trend like $CuCl_2$ and $NiCl_2$ based composite films. FTIR analysis inferring about the formation of β-phase in all the cases at lower and higher metal salt content. However the percentage of β-phase decline little bit at higher value of metal salt in all the cases ($CuCl_2$, $NiCl_2$, and $ZnCl_2$).These are preliminary information which further confirmed with XRD analysis.

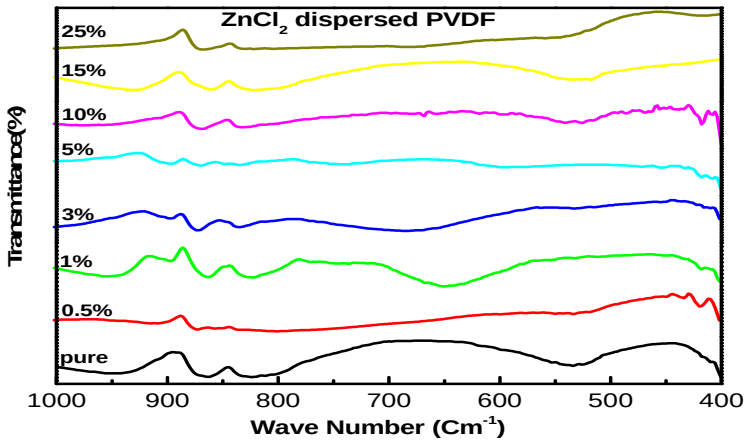

Figure 4.1 (C): FTIR spectra of PVDF-$ZnCl_2$ composite films at different concentrations (x=0.5, 1, 3, 5, 10, 15, and 25 wt %) casted from the mixed solvent solution (5:5 THF/DMF).

With allowance for the presence of different crystallographic phases, an attempt has been made to examine the β-phase of PVDF using tetrahydrofurane (THF) as swelling agent and dimethyalactamide (DMA) as a solvent. Figure 4.1 (d) shows the FTIR spectra of solution cast films derived from mixed solvents with m/m composition of THF/DMA at 5:5, 7:3, and 8:2, 9:1.

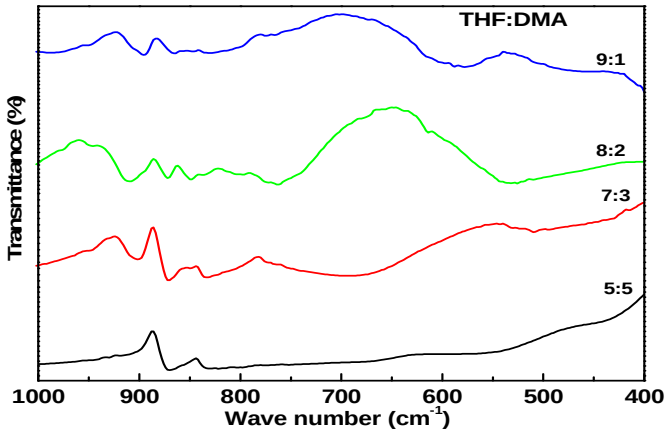

Figure 4.1(d): FTIR spectra of PVDF films casted from the mixed solvent solution with various mass ratio of THF/DMA (5:5, 7:3, 8:2, 9:1).

The bands observed at 510 and 845 cm^{-1} refers to the β-phase of PVDF. In all the four concentrations 7:3 THF/DMA concentration gives maximum amount of β-phase. This implies that highly polar solvents (i.e. the DMA composition increased) may induce the β

phase (TTTT) formation along with small reflection at 880 cm^{-1} indicate small amount of γ-phase. The β- and γ-phase are the most important phases their high polarizability facilitate many technological applications. These results confirming that DMA can also be used as solvent to tune PVDF crystalline phases. Though the DMA as a single solvent widely used to drive PVDF crystalline phase, but this is first time such phases observed in mixed solvent with DMA.

4.2. Structural analysis

Wide angle X-ray diffraction (WAXD) technique was used to identify the crystalline phase of pure and dispersed PVDF composite films. Figure [4.2 (a), 4.2 (b), 4.2 (c)] shows the XRD patterns of various transition metal salt ($CuCl_2$, $NiCl_2$, $ZnCl_2$) dispersed as synthesised PVDF composite films.

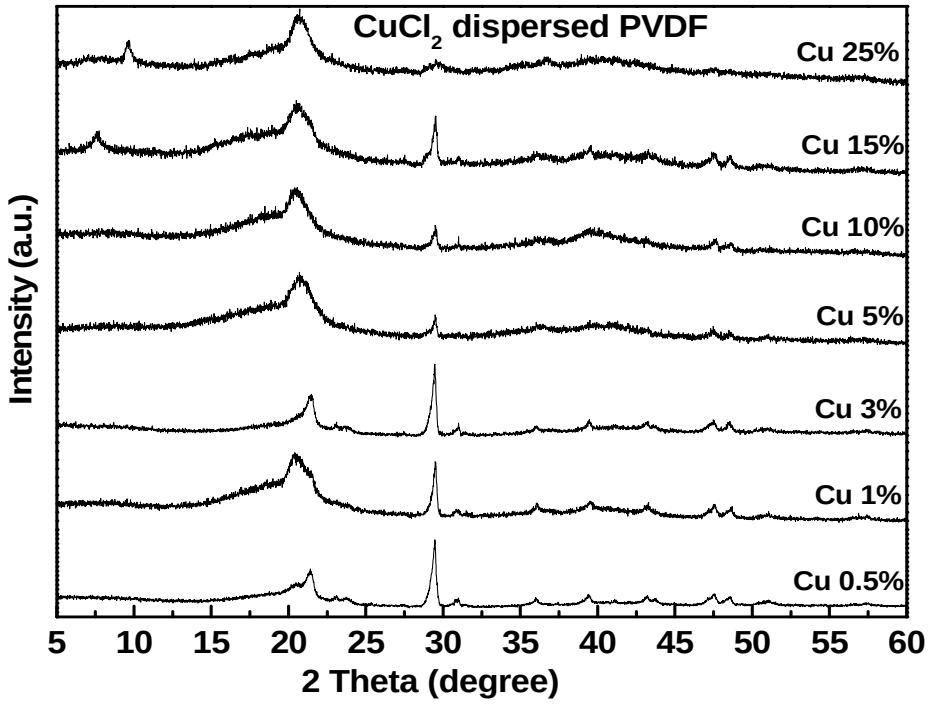

Figure 4.2(a): X-ray diffraction pattern of PVDF dispersed with various mass fractions of $CuCl_2$ (x=0.5, 1, 3, 5, 10, 15, and 25 wt %).

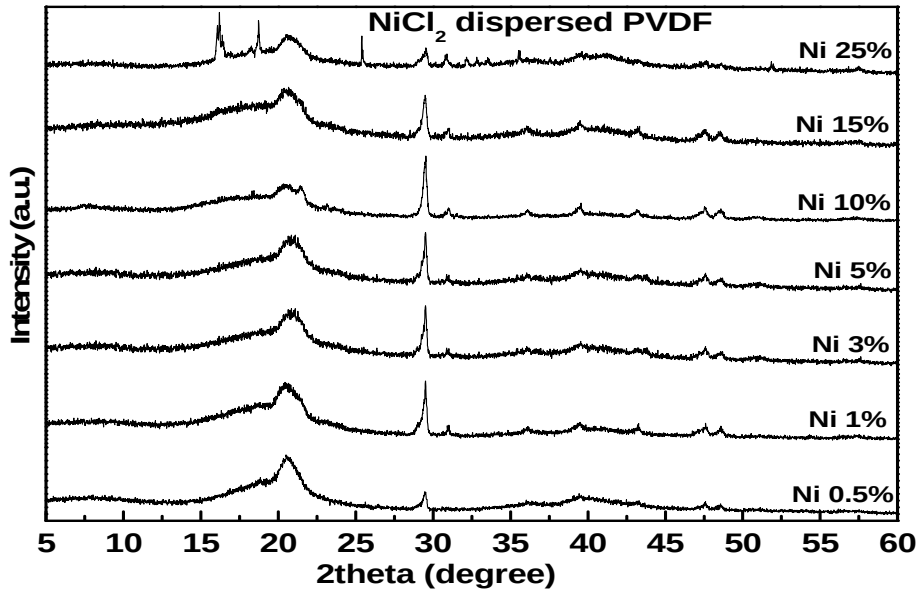

Figure 4.2 (b): X-ray diffraction pattern of PVDF dispersed with various mass fractions of $NiCl_2$(x=0.5, 1, 3, 5, 10, 15, and 25 wt %).

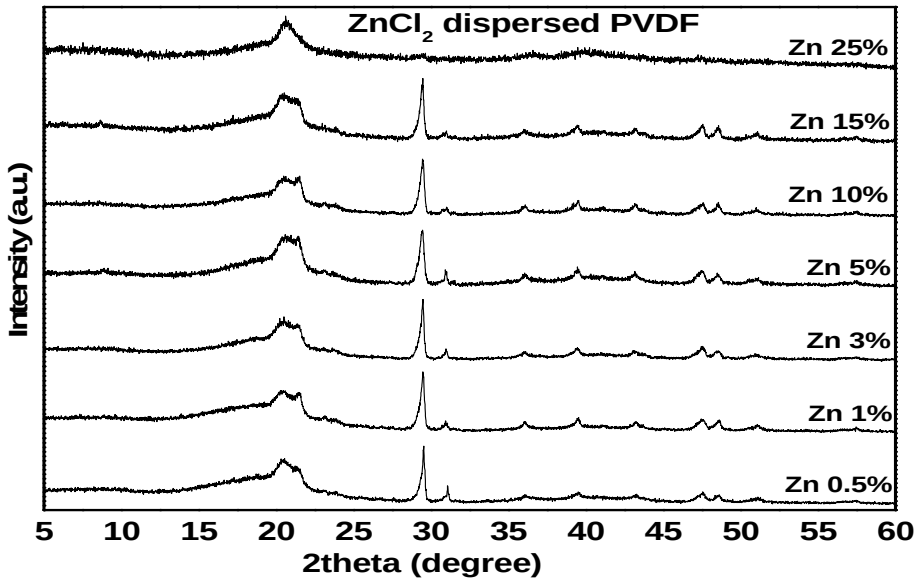

Figure 4.2 (c): X-ray diffraction pattern of PVDF dispersed with various mass fractions of $ZnCl_2$(x=0.5, 1, 3, 5, 10, 15, and 25 wt %).

All the samples were found crystalline in the nature as well-defined diffraction peaks are extended over 2θ scale up to higher intensity. The peaks observed for all the samples dispersed with ($CuCl_2$, $NiCl_2$, $ZnCl_2$) at 2θ=21° refer to the sum of diffraction planes (110) and (200) and the peak at 39° refer to the diffraction plane (002). These reflections correspond to the β-phase and γ-phase of PVDF respectively. However, some impurity peaks

were noticed at higher metal salt concentration in case of $NiCl_2$ as evident from the figure 4.2 (b). Note that one characteristic reflection at $2\theta=29°$ consistently appeared in all the samples. We fail to index this reflection as it does not correspond to the any phase of PVDF and metal salt. There is no information regarding this peak found in the literature also. XRD analysis, inferring that the metal salt well dispersed in the matrix of PVDF without disturbing the structure and also enhancing the β content in all these composite films.

The temperature and time of crystallization determine the presence of predominant phases in PVDF. The annealing conditions decide the presence of different phases and conversion of one phase to other phase of PVDF. The β-phase, which is important for ferroelectric applications, has been obtained from γ-phase by suitable annealing conditions. All the samples were heated at 90°C to check the effect of annealing on the crystalnity of the pure and TMS dispersed PVDF composite films. All the samples were found crystalline in nature as evident from the figure 4.2(d), (e) and (f) without any other phase formation.

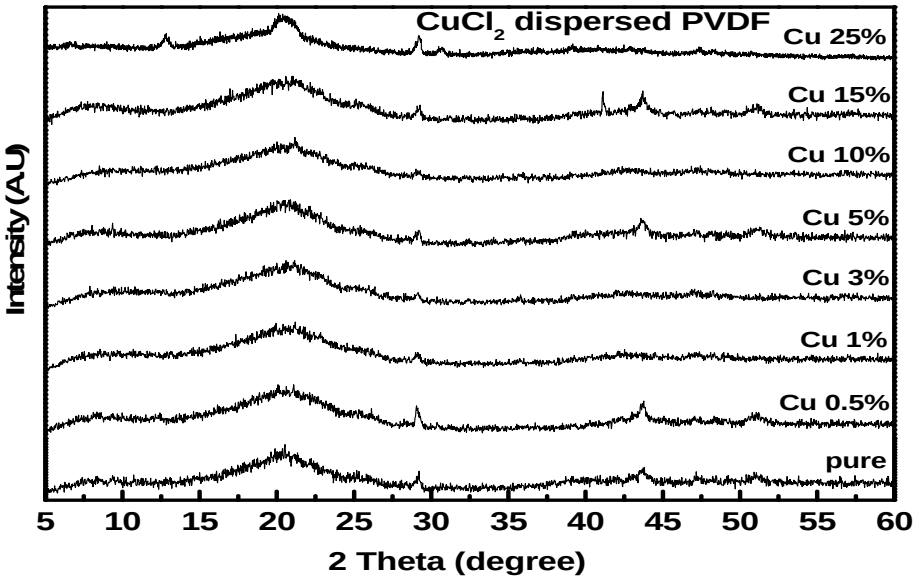

Figure 4.2 (d): X-ray diffraction pattern of PVDF dispersed with various mass fractions of $CuCl_2$ (x=0.5, 1, 3, 5, 10, 15, and 25 wt %) annealed at 90°C.

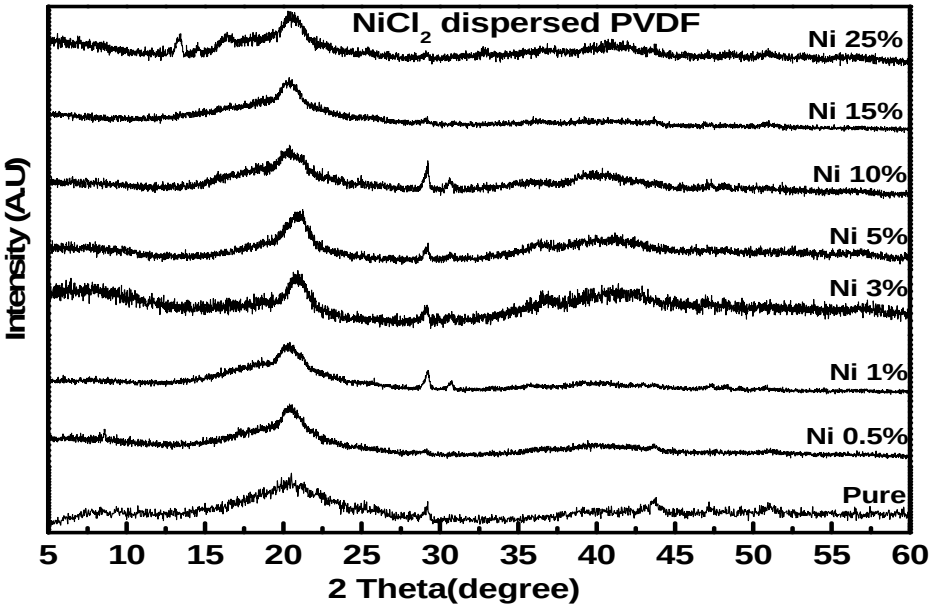

Figure 4.2 (e): X-ray diffraction pattern of PVDF dispersed with various mass fractions of $NiCl_2$(x=0.5, 1, 3, 5, 10, 15, and 25 wt %) annealed at 90°C.

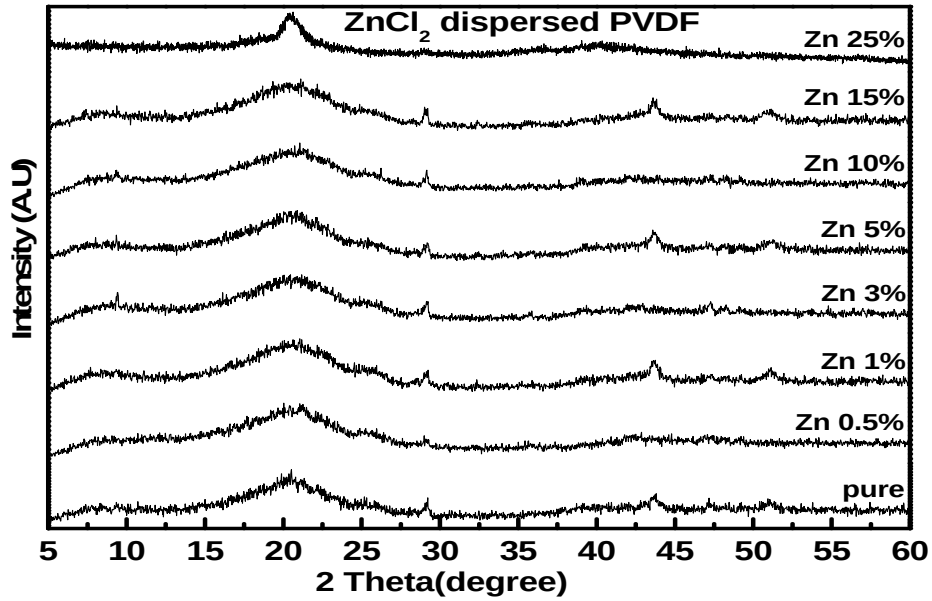

Figure 4.2 (f): X-ray diffraction pattern of PVDF dispersed with various mass fractions of $ZnCl_2$ (x=0.5, 1, 3, 5, 10, 15, and 25 wt %) annealed at 90°C.

The well defined peaks observed at 2θ=21° indicative of β-phase of PVDF consistently for all samples. Simultaneously some impurity peaks have been observed at Cu=25% and Ni=25%.

The diffraction peak at 2θ=29° also consistently observed for all the samples after annealing. Although, the intensity of this peak become negligible than that of as synthesized composite films. It is interesting to note that γ-phase eventually disappeared after annealing as no reflection observed at 2θ=39°, which was noticed in as synthesis samples. From above analysis it was concluded that annealing process increased the crystallnity in composite films along with the higher percentage of β content and diffuse other phases.

At annealing temperature 90°C for 5 hours the viscosity of material decreases but still high enough to prevent the orientation of crystals but the chain mobility increases enough to reorganize the structure of conformers. Since 90°c is just above α relaxation temperature the conversion rate from α to β-phase occurs due to motion of conformers without considerable deformation of the crystals. At this temperature crystallization rate of β phase is also higher among other phases. So after annealing the PVDF films at 90°C for 5 hours, the increase in β phase has been observed in it. In the β- phase of PVDF the long trans zigzag segments are connected to each other with skew bond or equivalent gauche-trans sequences. It clearly reflects that the temperature gradient plays important role in the phase change and crystallnity in PVDF.

Figure 4.2 (g) shows the XRD pattern of solution cast films derived from mixed solvents with m/m composition 5:5, 7:3, and 8:2, 9:1.of THF/DMA.

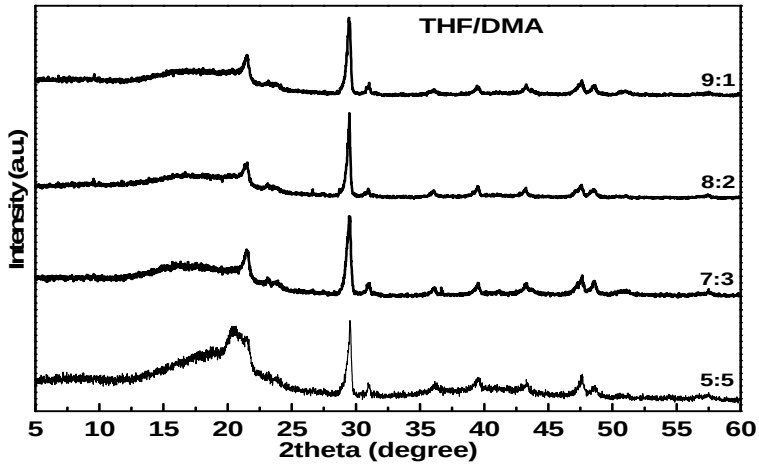

Figure 4.2 (g): XRD pattern of PVDF films casted from the various mass ratio of THF/DMA (5:5, 7:3, 8:2, 9:1).

The peak at 2θ=21° indicates the formation of pure β-phase. In all the four concentrations of THF/DMA the maximum percentage of β-phase is observed for 7:3. These results were in good agreement with FTIR observation. This implies that highly polar solvents (i.e. the DMA

composition increased) may also induce the β-phase (TTTT) as well as smaller amount of γ-phase as the diffraction peak observed at 2θ=39°. The XRD analysis reflects that DMA can be used as solvent with THF (swelling agent) to give the PVDF crystalline phase.

4.3 Conductivity measurement

The conductivity of transition metal salt ($CuCl_2$, $ZnCl_2$, and $NiCl_2$) dispersed PVDF composite films was calculated and plotted as a function of temperature in figure 4.3 (a), (b) and (c).

4.3.1 $CuCl_2$-PVDF composite film

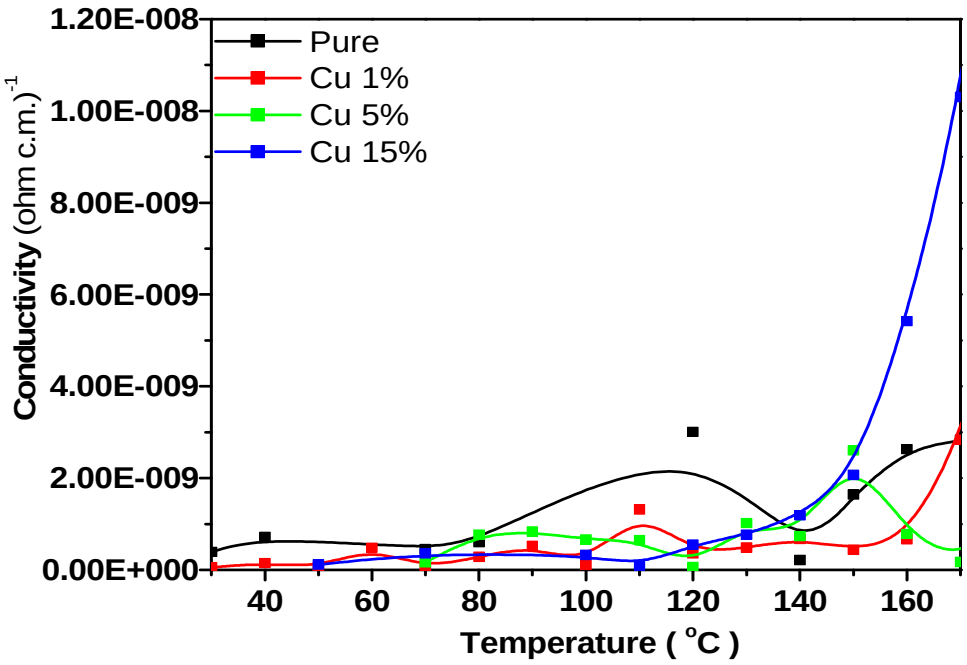

Figure 4.3 (a): Conductivity measurement of PVDF-$CuCl_2$ system with temperature.

From figure 4.3 (a) it is clear that the conductivity increase with increasing temperature for all samples. This can be explained with the help of free volume theory [25]. As the temperature increases, the polymer can expand easily and produce free volume. Thus ions, solvated molecules or polymer segments can move to the free volume and hence the increase in conductivity. The ion transport in polymer/filler depends on the polymer segmental motion [26].

4.3.2 $NiCl_2$-PVDF composite film

The conductivity variation of $NiCl_2$ dispersed PVDF composite film was shown in figure 4.3 (b).

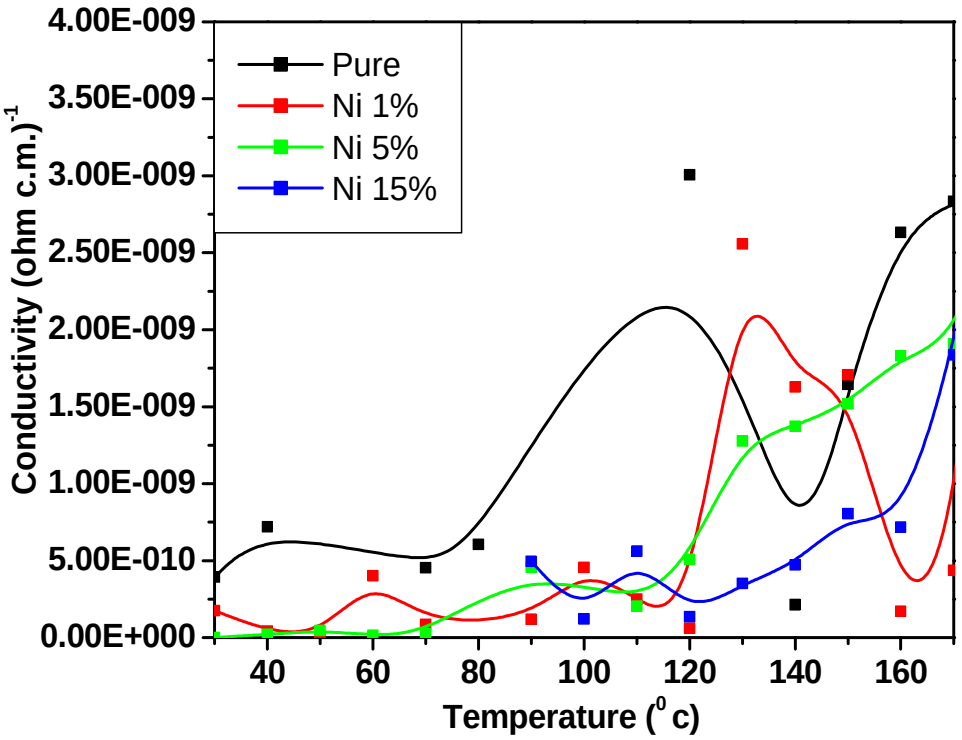

Figure 4.3 (b): Conductivity measurement of PVDF-$NiCl_2$ system with temperature.

In this case the conductivity does not show any significant change as system display decrease in the magnitude of conductance than that of pure PVDF at all concentration near 160°C. This behaviour in these films may attribute to the magnetic nature of $NiCl_2$.

4.3.3 $ZnCl_2$-PVDF composite film

The variation of conductivity as a function of temperature for $ZnCl_2$ dispersed PVDF films presented in the figure 4.3 (c). The composite films follow the same trend as $CuCl_2$ conductivity. It was found that the conductance of the system is increased at lower concentration and then decline at higher value of $ZnCl_2$.However, the net magnitude remain higher than that of pure PVDF film.

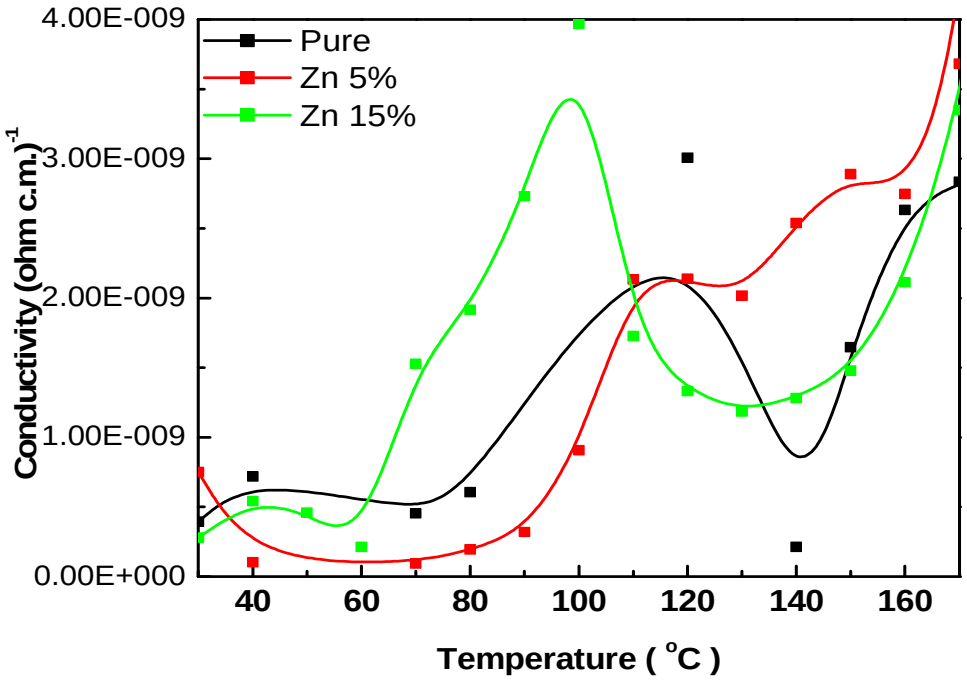

Figure 4.3 (c): Conductivity measurement of PVDF-$ZnCl_2$ system with temperature.

From the above conductivity analysis it can be concluded that such enhancement in the conductivity may attributed to the one dimensional phonon-assisted charge carrier hopping between poloran and/or bipolaron found state in the PVDF. It seems that the physical properties of the transition metal salt also play a vital role in conduction process. Such conducting composite films can be used to many technological applications.

4.4 Resistivity measurements

The resistivity of the synthesised sample as a function of different concentration of $CuCl_2$, $NiCl_2$ and $ZnCl_2$ metal salt were characterized in order to understand that exact mechanism of conduction or support the conduction in these systems.

4.4.1 $CuCl_2$-PVDF composite films

Figure 4.4 (a) displaying the variation of resistivity of $CuCl_2$ dispersed PVDF composite films as a function of temperature. It was found that the resistivity of thin films was maximum at lower temperature and become minimum near melting transition of PVDF. We observed that the resistivity at lower value of $CuCl_2$ was maximum and then decline at higher concentration in lower temperature region.

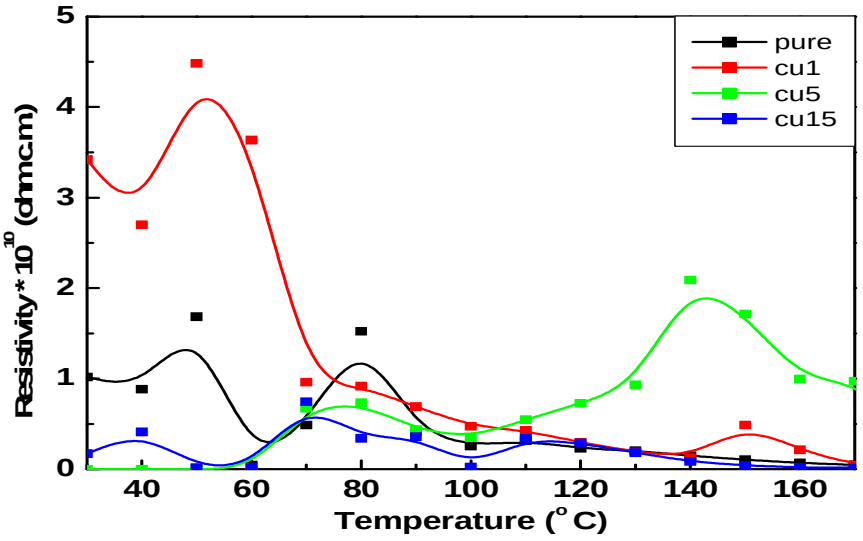

Figure 4.4 (a): Variation of resistivity of PVDF-$CuCl_2$ system with temperature.

However, higher temperature zone resistivity shows maximum magnitude for 5 wt%. These results were also supporting the conductivity observations.

4.4.2 $NiCl_2$-PVDF composite films

Figure 4.4 (b) presenting the variation of resistivity of $NiCl_2$ dispersed PVDF composite films with temperature.

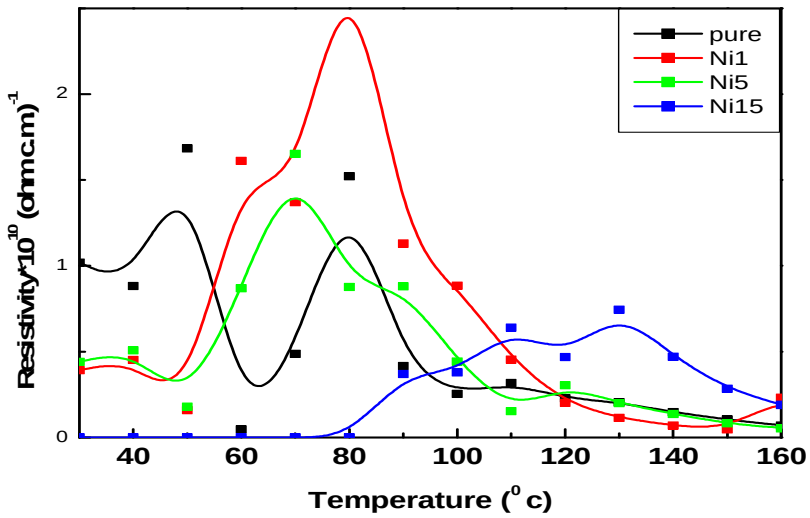

Figure 4.4 (b): Variation of resistivity of PVDF -$NiCl_2$ system with temperature

These films showing same trend as $CuCl_2$ dispersed films. It was found that resistivity first rise at lower concentration of transition metal salt and then decreases as reach to higher value of $CuCl_2$ in lower temperature region. However the resistivity of all the samples was found minimum near melting temperature of PVDF.

4.4.3 $ZnCl_2$-PVDF composite films

The variation of resistivity as a function of temperature in $ZnCl_2$ dispersed PVDF films is shown in figure 4.4 (c)

.

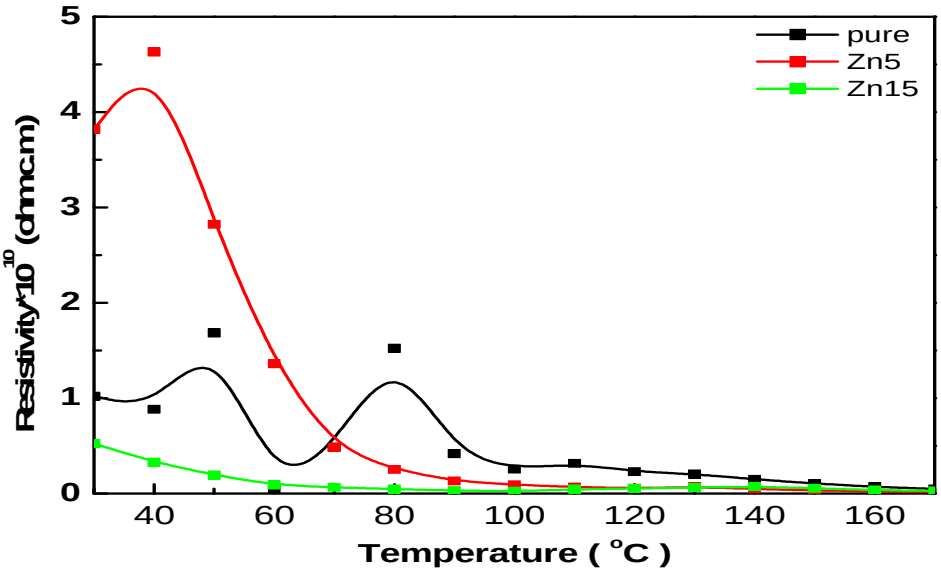

Figure 4.4 (c): Variation of resistivity of PVDF -$ZnCl_2$ system with temperature.

The resistivity of 5wt% concentration was found maximum and then decline at higher metal salt content in the lower temperature region. However, at higher value of temperature the resistivity becomes negligible. Such variation of resistivity supported the conductivity of all the samples.

4.5 Calorimetric measurements

The thermodynamical characterization of pure and transition metal salt dispersed PVDF composite films were carried out using DSC (LINSIS L-63), in order to understand the variation of thermal parameter in the presence of transition metal salt and their corresponding effect on physical properties.

The DSC spectra of pure and $CuCl_2$ dispersed composite films are shown in the figure 4.5 (a). We observed that the endotherm near 160°C for pure PVDF samples indicating the melting transition of PVDF. The broadening in the peak corresponds to the melting fraction of entangled polymer chain.

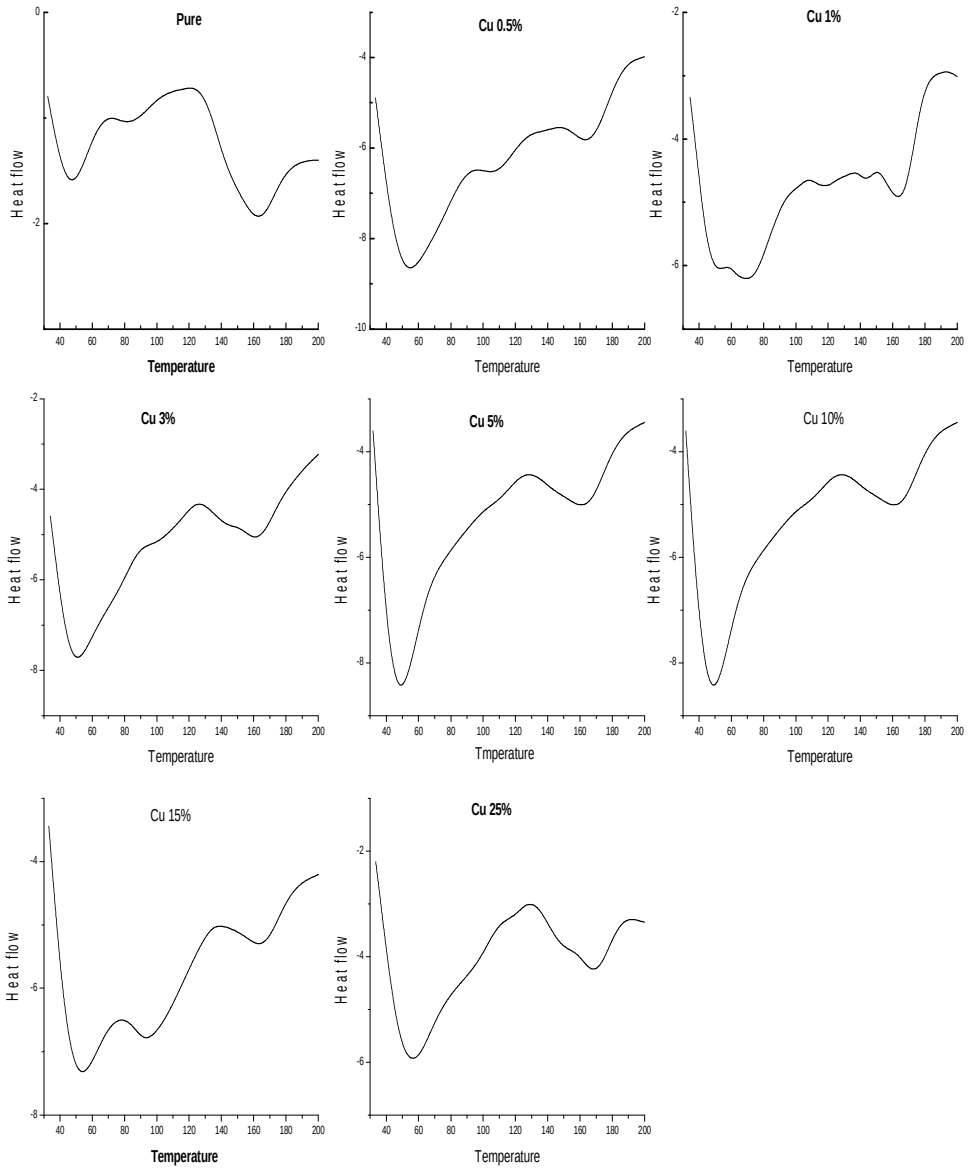

Figure 4.5 (a) DSC profiles of pure and $CuCl_2$ dispersed PVDF films at different concentration of $CuCl_2$.

The transition temperature was found to increase at lower concentration with the addition of $CuCl_2$ and then decline to lower value up to 10 wt%. However, at higher transition metal salt concentration melting temperature shifts to higher value. Such shift in the melting temperature may be due to the induction of some degree of ordering in the presence of transition metal salt.

Similarly the DSC spectra of $NiCl_2$ dispersed PVDF composite films is shown in figure 4.5 (b).

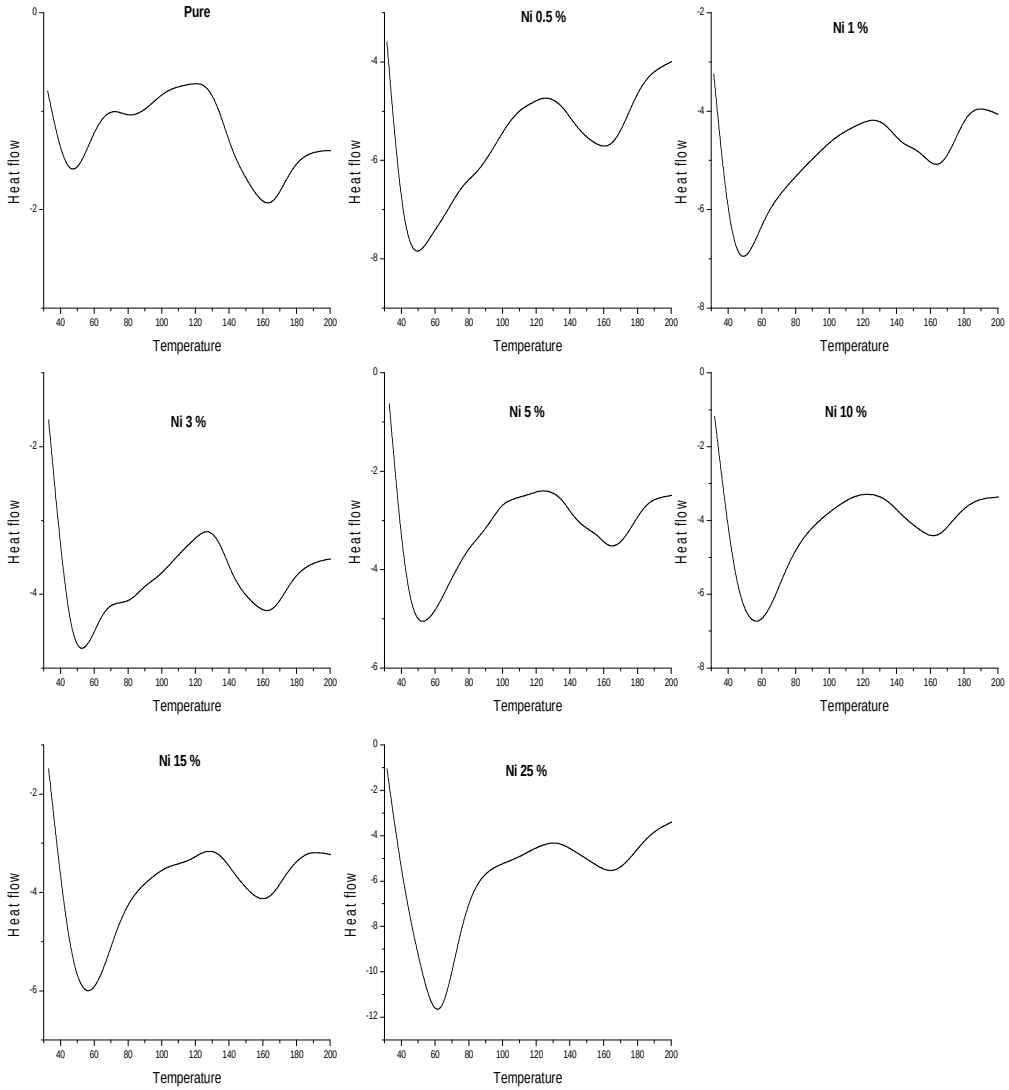

Figure 4.5 (b) DSC profiles of pure and $NiCl_2$ dispersed PVDF films at different concentration of $NiCl_2$.

The variation in transition temperature ranging between 158.5-163.6°C has been noticed for these films. However these melting transitions did not display any regular trend.

In the same way the DSC of the $ZnCl_2$ dispersed PVDF composite films is presented in the figure 4.5 (c)

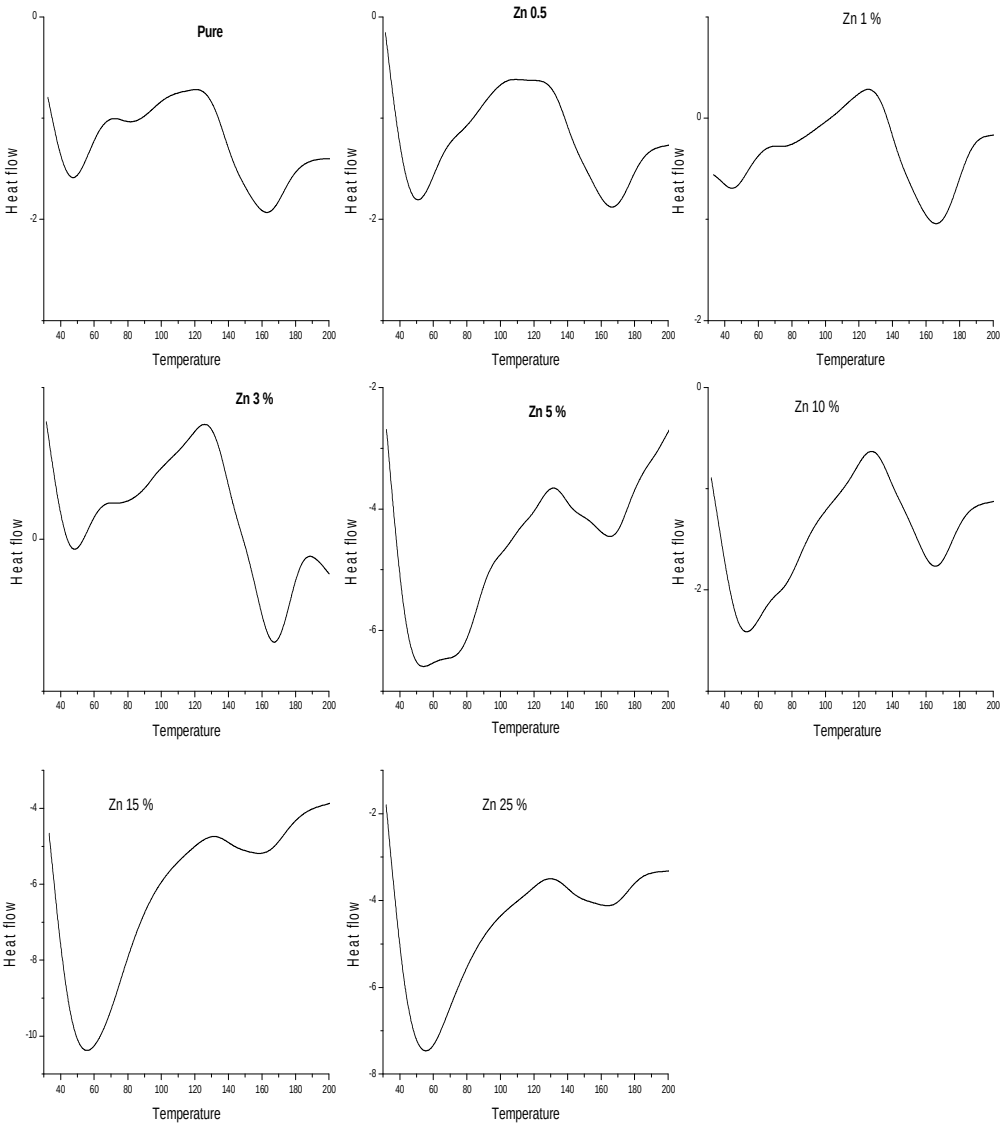

Figure 4.5(c) DSC profiles of pure and $ZnCl_2$ dispersed PVDF films at different concentration of $ZnCl_2$.

We observed that the melting temperature shift to higher side than that of pure one as it display melting temperature around 162°C consistently up to 10 wt% and then fall to lower value at higher metal salt concentration.

The variation of melting point with concentration for their endotherm observed for $CuCl_2$, $NiCl_2$ and $ZnCl_2$ dispersed PVDF films are displayed in figure 4.5(d).

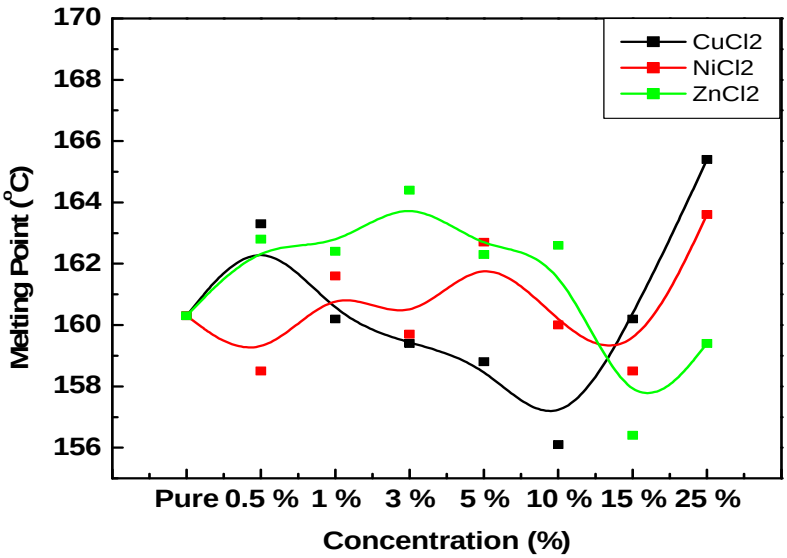

Figure 4.5(d): Variation of melting temperature with different metal salt concentrations.

Table:4.5.1 Variation of melting temperature with different metal salt concentration.

Sr.No.	Conc. ⇨ Salt ⇩	Pure	0.5 wt%	1 wt%	3 wt%	5 wt%	10 wt%	15 wt%	25 wt%
1.	$CuCl_2$	160.3	163.3	160.2	159.4	158.8	156.1	160.2	165.4
2.	$NiCl_2$	160.3	158.5	161.6	159.7	162.7	160.0	158..5	163.6
3.	$ZnCl_2$	160.3	162.8	162.4	164.4	162.3	162.6	156.4	159.4

Thermal parameter, entropy was also calculated for the endotherm observed at various transition metal salt dispersed composite films is listed in table 4.5.2 below and plotted in the figure 4.5(e) respectively.

Table:4.5.2 variation of entropy with different metal salt concentration.

Sr.No.	Conc. ⇨ Salt ⇩	Pure	0.5 wt%	1 wt%	3 wt%	5 wt%	10 wt%	15 wt%	25 wt%
1.	$CuCl_2$	0.5644	0.2160	0.0980	0.1094	0.1175	0.0174	0.0802	0.4587
2.	$NiCl_2$	0.5644	0.3266	0.1532	0.3264	0.2295	0.3199	0.2539	0.3711
3.	$ZnCl_2$	0.5644	0.3537	0.4151	0.3876	0.3054	0.2490	0.1864	0.1600

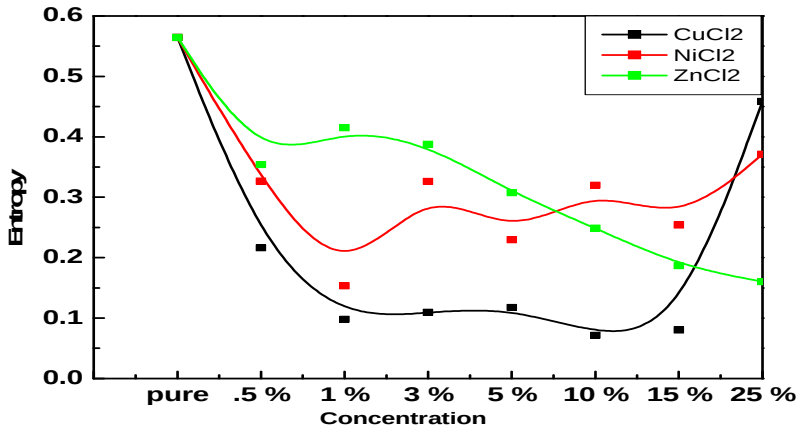

Figure 4.5(e): Variation of entropy with different metal salt concentrations.

It was found that the entropy of pure PVDF film was higher than that of dispersed composite films. In case of $ZnCl_2$-PVDF composite films, the entropy fall with the addition of small amount of metal salt and preserve this behaviour up to 15 wt%. Further increase in the concentration gives rise in the entropy of the system. Such behaviour reflects that the addition of $CuCl_2$ induce some degree of ordering in the system up to 15 wt% concentration. Film dispersed with $NiCl_2$ also shows decrease in entropy at lower concentration, but shows some peculiar behaviour with increase in the transition metal salt concentration (as many crust and trough were observed). However $ZnCl_2$ dispersed PVDF composite films display decrement in entropy with rise in metal salt content up to higher value but having higher magnitude than other two. The observed trend was $NiCl_2 > CuCl_2 > ZnCl_2$. These results were found in good correlation with the XRD analysis.

4.6 Morphological analysis

The pure and transition metal salt dispersed composite films were characterized using SEM. The observed micrograph shown in figure 4.6[(a), (b), (c)] respectively for $CuCl_2$, $NiCl_2$, $ZnCl_2$ dispersed thin films at 1, 5, 15,25wt%. It was found that the fine spherulites were arranged in well defined fashion in all cases. It is evident from the SEM images that the $CuCl_2$ and $ZnCl_2$ dispersed samples were more porous than that of $NiCl_2$ loaded films.

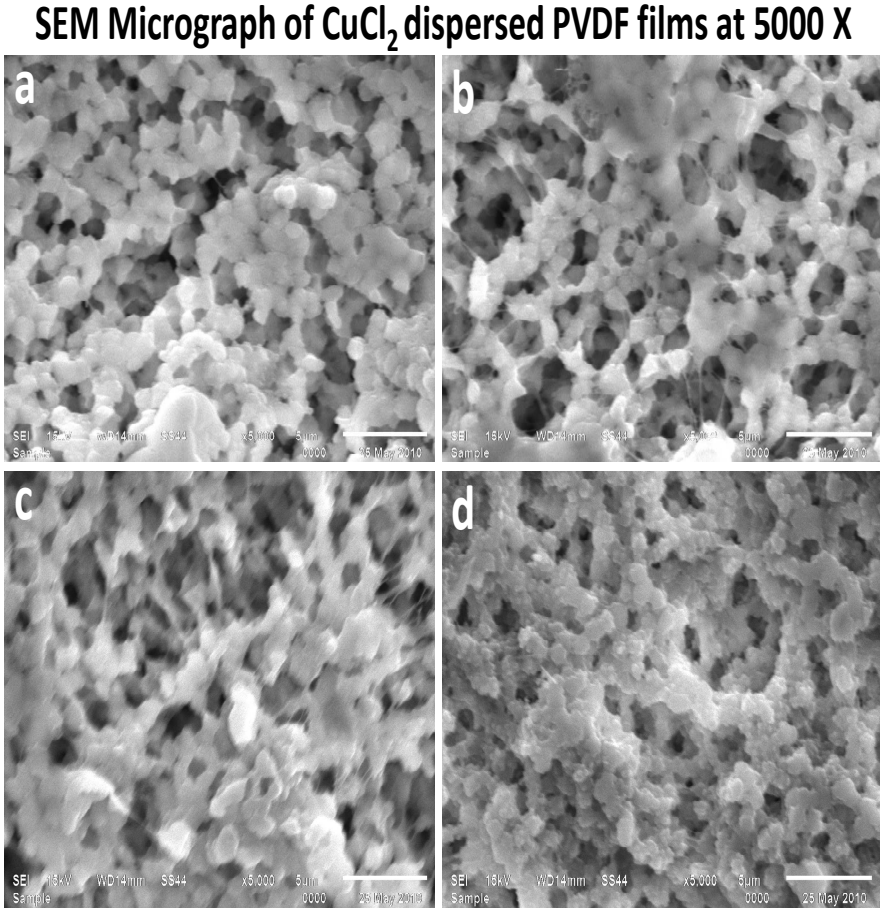

Figure 4.6 (a): SEM micrograph of $CuCl_2$ dispersed PVDF films.

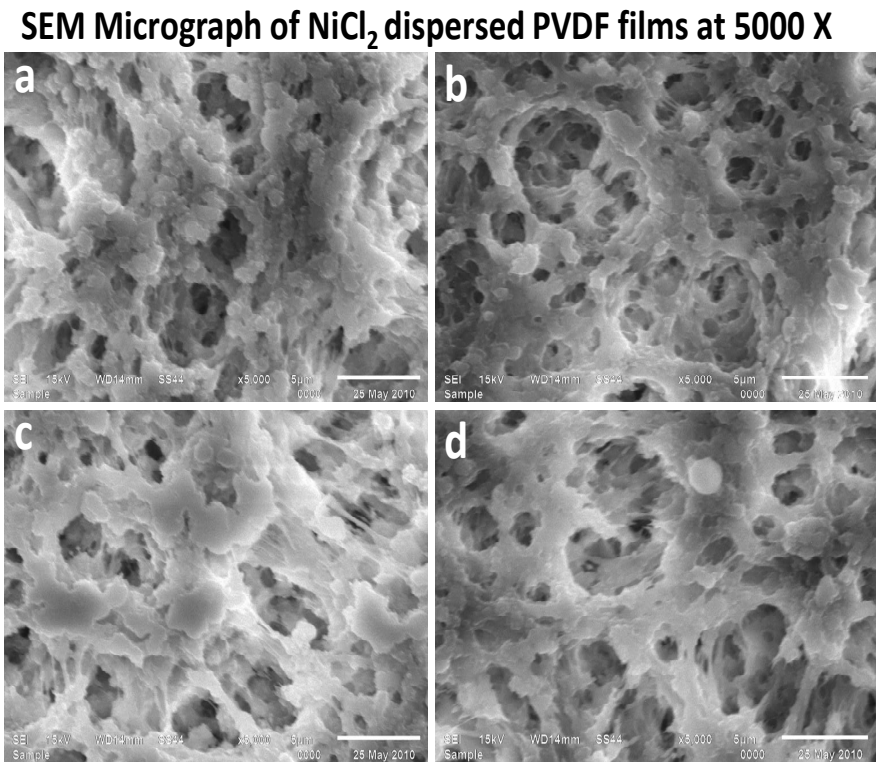

Figure 4.6 (b): SEM micrograph of $NiCl_2$ dispersed PVDF films.

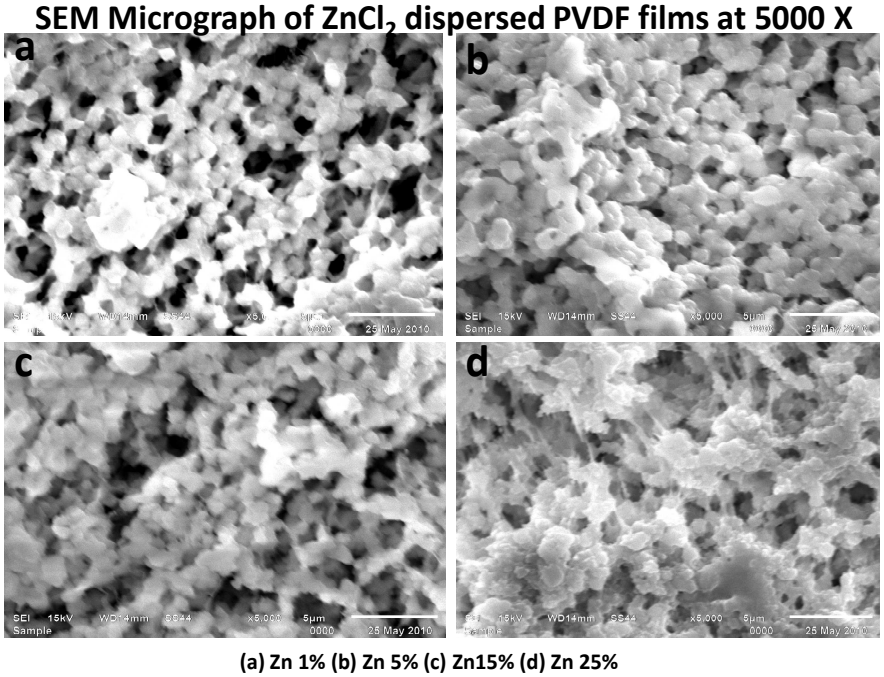

Figure 4.6 (c): SEM micrograph of $ZnCl_2$ dispersed PVDF films.

4.7 Dielectric Studies

The temperature and frequency dependent dielectric behaviour of pure and metal salt dispersed PVDF composite films in the frequency range 50Hz to 1MHz has been studied.

4.7.1 Dielectric study of PVDF-$CuCl_2$ composite (Thin Films)

Frequency and temperature dependence of relative permittivity

The relative permittivity as a function of frequency for different concentration of $CuCl_2$ at 160°C near melting transition is shown in figure 4.7 (a).

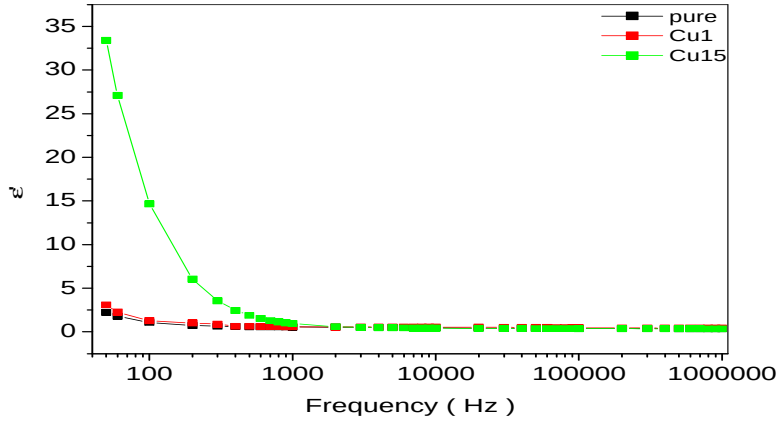

Figure 4.7 (a): variation of dielectric constant as function of frequency for PVDF-$CuCl_2$ composite films at 160°C.

It was observed that the dielectric constant gradually increase with variation of $CuCl_2$ concentration and shows higher magnitude at 15 wt% at lower frequency. However dielectric constant decline with increment in frequency and becomes low at higher frequency range.

Figure 4.7 (b) represents the dielectric loss for the $CuCl_2$ dispersed PVDF films.

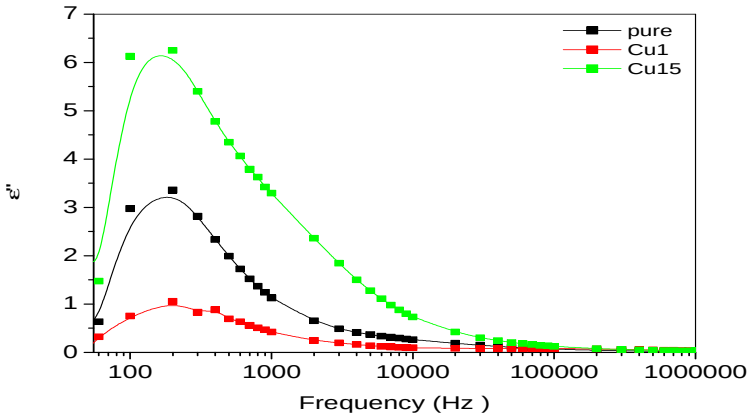

Figure 4.7 (b): Dielectric loss as function of frequency for PVDF-$CuCl_2$ composite films at 160°C.

We observed that the dielectric loss decrease with $CuCl_2$ addition and then become maximum at higher concentration. Such variation may be due to the higher metal salt density at higher concentration.

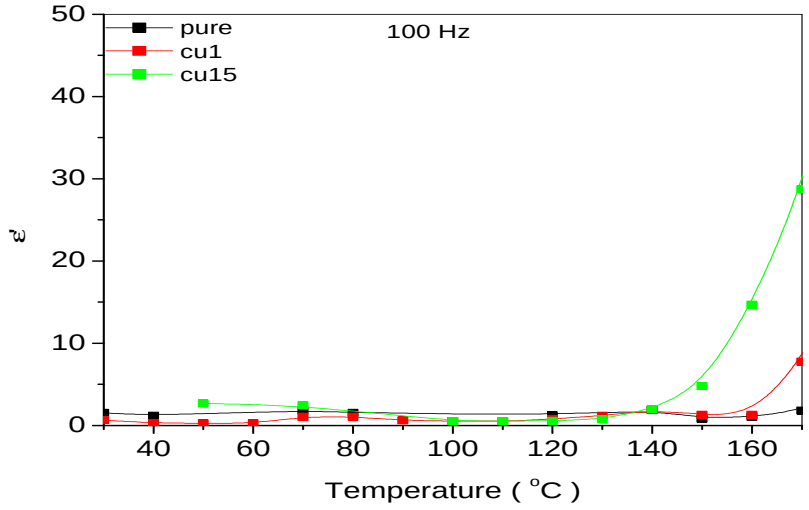

Figure 4.7 (c): Variation of relative permittivity with temperature at different concentrations of $CuCl_2$.

The temperature dependent variation of relative permittivity at 100Hz for PVDF-$CuCl_2$ composite system for (pure, 1, 15) concentration is shown in the figure 4.7 (c).

It was noted that the dielectric constant increased consistently with increment in the metal salt concentration. Similarly the value of loss factor for the system is presented in the figure 4.7 (d).

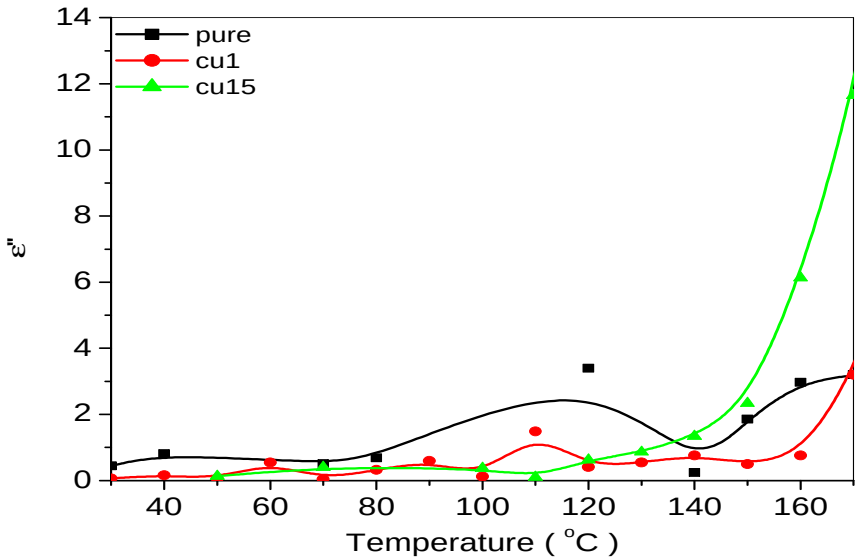

Figure 4.7 (d): Variation of dielectric loss with temperature at different concentrations of $CuCl_2$.

It was found that losses are smaller for lower concentration and consistently increased at higher metal salt concentration.

Dielectric study of PVDF-$NiCl_2$ composite (Thin Films)

Frequency and temperature dependence of relative permittivity

The variation of the relative permittivity as a function of frequency for different concentration of $NiCl_2$ is shown in figure 4.7 (e). It was found that the no subsequent variation in the dielectric constant has been found in the samples. The observed magnitude at all these concentrations is about same as pure PVDF.

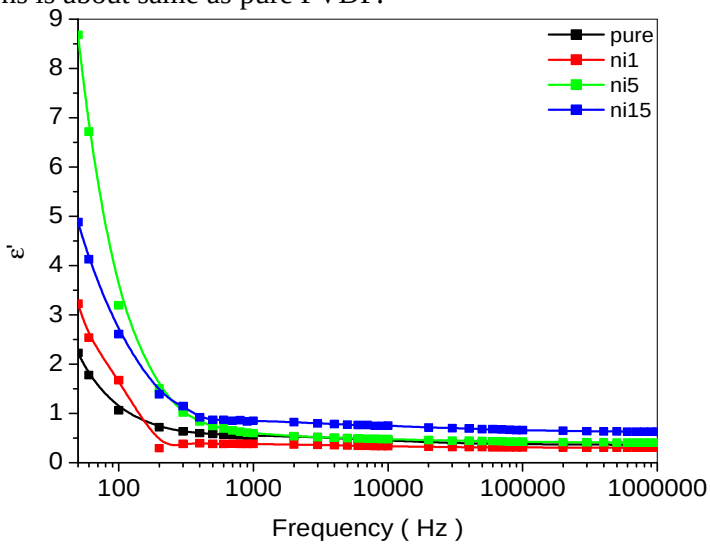

Figure 4.7(e): variation of dielectric constant as function of frequency for PVDF-$NiCl_2$ composite films at 160°C

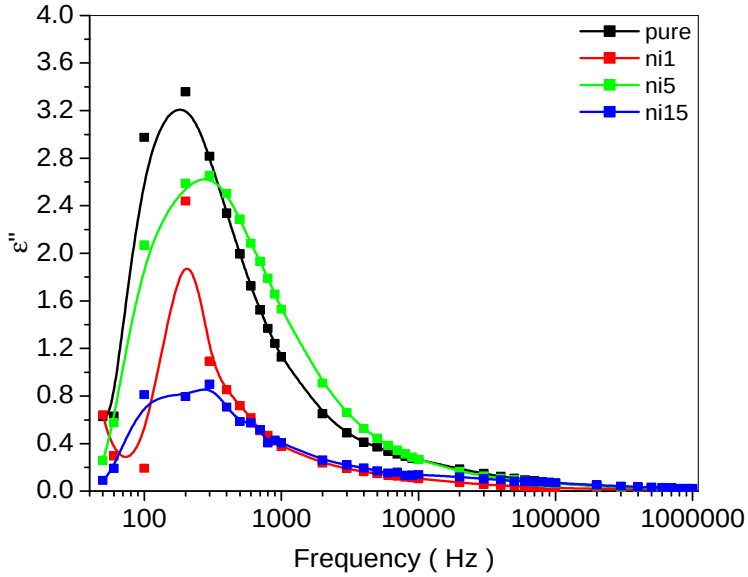

Figure 4.7 (f): Dielectric loss as function of frequency for PVDF-$NiCl_2$ composite films at 160°C.

Figure 4.7(f) shows the variation of dielectric loss as function of frequency. It was noticed that dielectric loss become minimum with addition of TMS. The gradual decreases in the loss factor have been observed with the increasing concentrations.

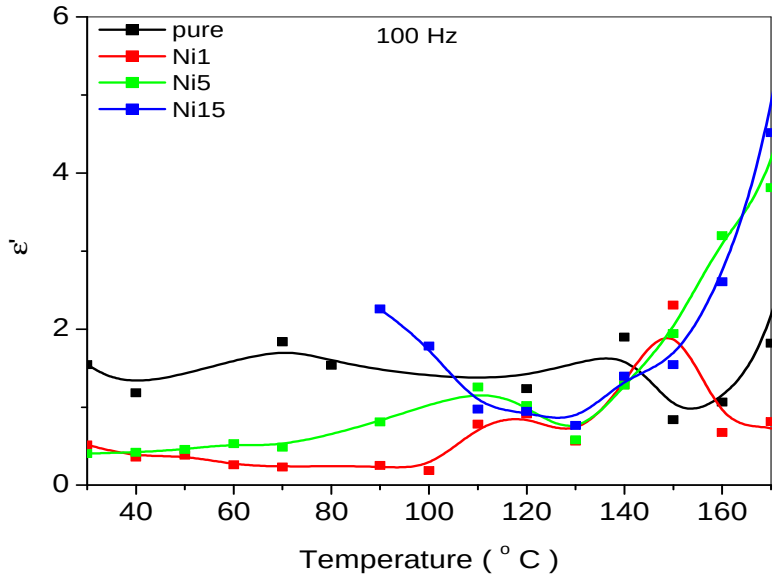

Figure 4.7(g): Variation of relative permittivity with temperature at different concentrations of $NiCl_2$ in PVDF at 100 Hz.

Figure 4.7(g) shows the variation of dielectric constant as function of temperature. No significant change has been found as the magnitude of the dielectric constant was same as pure PVDF.

Figure 4.7 (h) show the variation of losses as a function of temperature. We found that loss factor decreases with increase in the concentration of $NiCl_2$ near melting temperature.

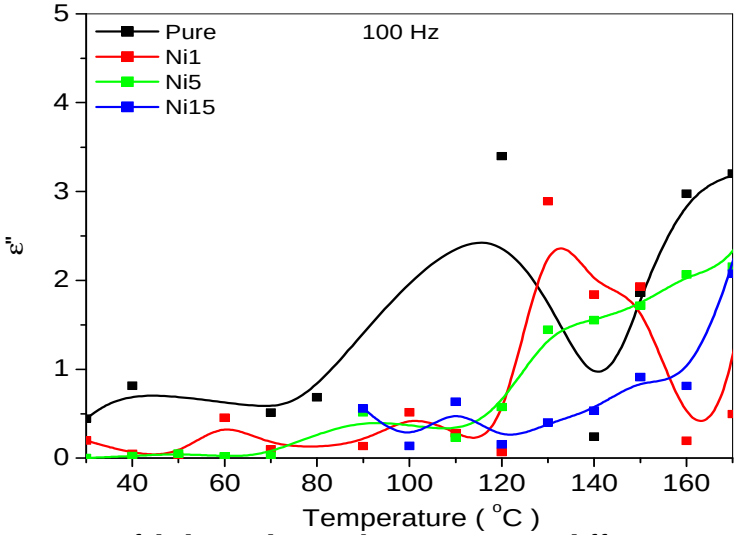

Figure 4.7 (h): Variation of dielectric loss with temperature at different concentrations of $NiCl_2$ in PVDF at 100 Hz.

Dielectric study of PVDF-$ZnCl_2$ composite (Thin Films)

Frequency and temperature dependence of relative permittivity

Figure 4.7 (i) show the variation of relative permittivity as a function of frequency for different concentration of $ZnCl_2$ at 160°C.

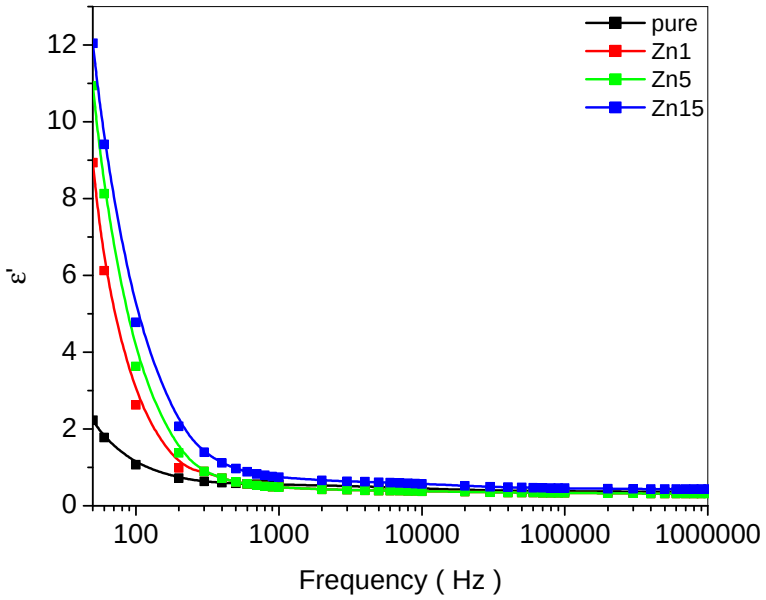

Figure 4.7 (i): variation of dielectric constant as function of frequency for PVDF-$ZnCl_2$ composite films at 160°C.

We observed that that the dielectric constant generally increased with the addition of metal salt up to higher concentration. However magnitude remains the same as pure PVDF. Such behaviour attributed to the fact that $ZnCl_2$ is metallic in nature which enhances the conductivity and decreases the dielectric constant.

Figure 4.7 (j) shows variation of dielectric loss as a function of frequency for all concentration of $ZnCl_2$. We observed that the dielectric loss decreased with increased in the metal salt concentration at lower value and then increased at intermediate value. However at higher value the value of losses again decreased at higher metal salt concentration.

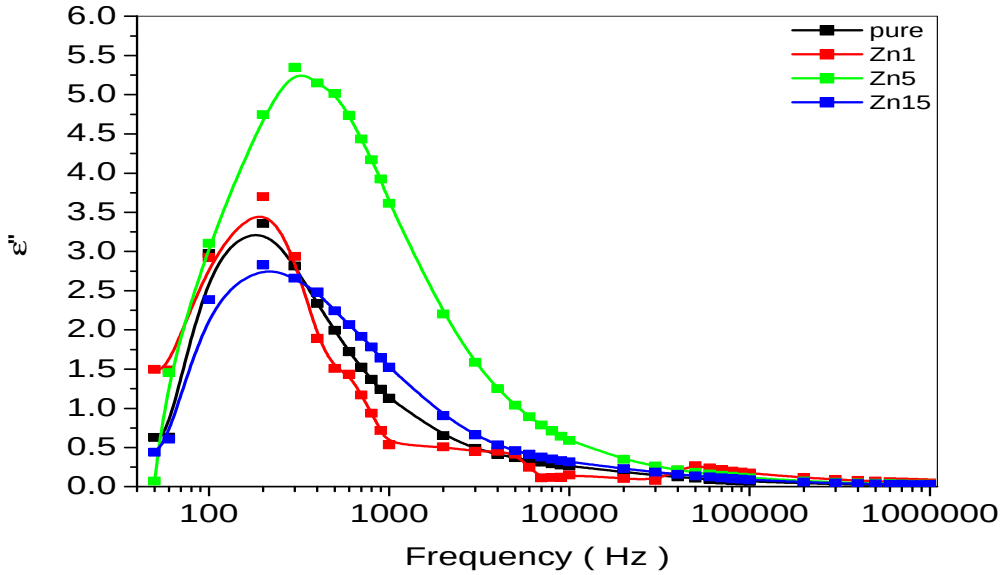

Figure 4.7 (j): Dielectric loss as function of frequency for PVDF-$ZnCl_2$ composite films at 160°c.

Figure 4.7 (k) shows the variation of dielectric constant as a function of temperature. We have noticed that dielectric constant increased at lower value of metal salt concentration and then decreased at higher concentration.

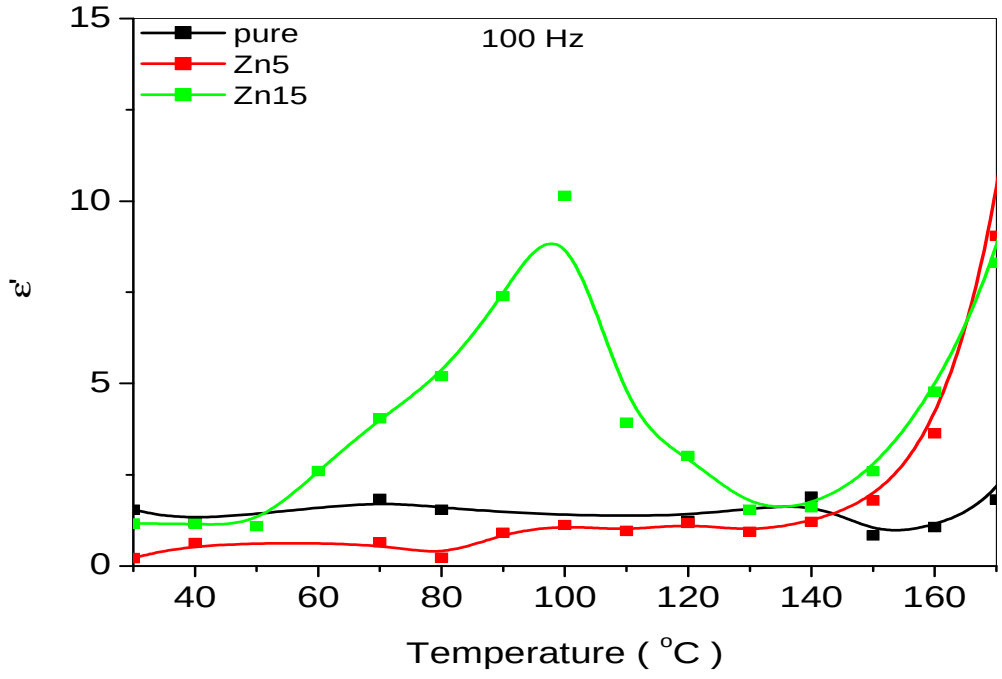

Figure 4.7 (k): Variation of relative permittivity with temperature at different concentrations of $ZnCl_2$ in PVDF at 100 Hz.

Value of dielectric loss at 100 Hz as a function of temperature for $ZnCl_2$ dispersed PVDF films are shown in figure 4.7 (l). We observe that the losses are increased with the variation of transition metal salt concentration.

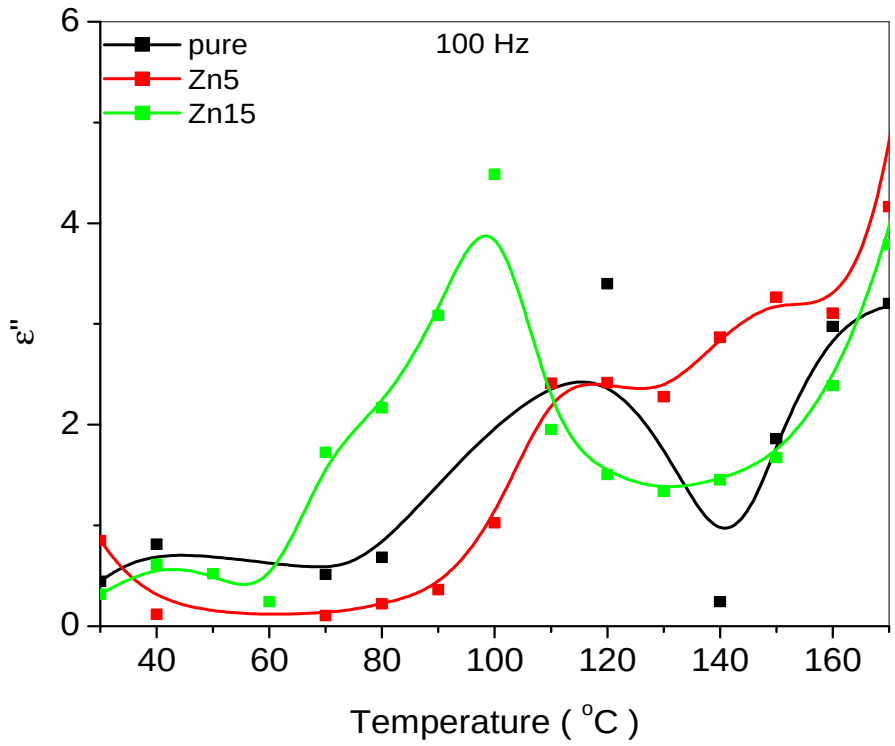

Figure 4.7 (l): Variation of dielectric loss with temperature at different concentrations of $ZnCl_2$ in PVDF at 100 Hz.

From the dielectric analysis it concludes that there is no significant variations have been found with the addition of transition metal salt. The magnitude of the dielectric constant is same as pure PVDF. Only one peculiar variation of dielectric constant was obtained at 15 wt% of $CuCl_2$ which shows higher magnitude than that of pure PVDF.

CONCLUSIONS AND FUTURE SCOPE

CONCLUTIONS

1. In summary, we have successfully synthesized TMS- PVDF composite systems via mixed solvent route. Which display β crystalline phase in as synthesized and annealing conditions with higher percentage.
2. Chemical analysis gives preliminary signature of the β-phase formation in all cases of transition metal salt dispersed composite films.
3. The formation of pure well crystalline β-phase has been confirmed from the XRD analysis up to higher percentage of the TMS. It was concluded that the addition of TMS did not disturb the crystal structure of PVDF and the filler materials was well dispersed in the host matrix. Though, negligible amount of impurity peak was observed at the 25 wt% concentration of $NiCl_2$. One consistent peak in all cases appeared at $2\theta = 29^0$. It is being investigated as it does not correspond to the crystal structure of host and filler material.
4. The conductivity calculated for these systems shows the increment with the increase in the TMS concentrations up to higher density. The magnitude of the conductance was found higher than that of pure PVDF in all cases. Such polymeric flexible matrixes with higher conductivity can be utilized in the field of electronics. The resistivity obtained for these composite systems was also in good correlation with these results.
5. Morphological investigations suggesting that the small spherulites are arranged in well ordered fashion in all the composite films. Films loaded with $CuCl_2$ and $ZnCl_2$ were found more porus than that of $NiCl_2$ dispersed composite films.
6. The calorimetric transitions displaying one melting transition in all the cases in the range 158-165^{0}C. However, softening of the sample start around 145^{0}C. The entropy for these found minimum in case of $CuCl_2$ loaded films and increases for $NiCl_2$ and $ZnCl_2$ systems.
7. The dielectric constant of these composite films was found same as pure PVDF; no significant variation has been noticed in any case except 15wt% loaded PVDF film which shows the dielectric constant around 34.

FUTURE SCOPE

A new area of research that has begun is in the area of soft multiferroic materials. Multiferroics are materials that simultaneously exhibit two or more "ferro" properties, i.e. ferroelectricity, ferromagnetism, or ferroelasticity. With ferroelectric polymers, such as poly (vinylidene difluoride) (PVDF), we may be able to create composites that could be multiferroic. By doping PVDF with magnetic transition metal ions we hope to induce a coupling between the magnetic moment of the transition metal with the electric moment of the polymer. Further, the ionic salt also induces the PVDF to crystallize in the ferroelectric β-phase.

REFERENCES

[1]. Glushanin, S.; Topolvo, V.; Krivoruchko, A. V.; “Features of piezoelectric properties of 0-3 PbTiO3-type ceramic/polymer composites”, *Materials Chemistry and Physics* 97 (2-3), 357-364, (2006).

[2]. Elashmawi, I.S.; “Effect of NaCl filler on ferroelectric phase and polaron configurations of PVDF films”, *Cryst. Res. Technol.* 42, 389-393, (2007).

[3]. Yoon, Sun.; Prabu, Arun Anand.; Kim, Kap Jin.; Park, Cheolmin.; “ Metal salt Induced Ferrolectric Crystalline Phase in PVDF Films”, *Macromolecular Rapid Communications* 29, 1316-1321, (2008).

[4]. Ma, Wenzhong.; Zhang, Jun.; Chen, Shuangjun.; Wang, Xiaolin.; “Crystalline Phase Formation of PVDF from THF/DMF Mixed Solution”, *Journal of Macromolecular Science, Part B: Physics*, 47, 434-449, (2008).

[5]. Pennnings, A.J.; Kiel, A.M., Kolloid, Z.Z.; *Polymer*, 160, 205, (1965).

[6]. Andrew J. Lovinger.; “Ferroelectric Polymers”, *Sciences* 220, 1115-1121, (1984).

[7]. H. Sussner and K. Dransfeld.; “Importance of the metal-polymer interface for the piezoelectricity of PVDF”, *J. Polymer. Sci. Polym. Phys*,16, 529, (1978).

[8]. Bernasconi J., ‘ Conduction in anisotropic disorder system: Effective-medium theory’, *Physical Review B:* Vol 9, No. 10, (1974).

[9]. Broadhurst MG, Davis GT J Appl Physics 49:4992 (1978).

[10]. Ma WZ, Zhang XL, Wang SM Appl Surf Sci 253:8377, (2007).

[11]. Wenzhong Ma E Jun Zhang E Xiaolin Wang, J Mater Sci 43:398-401, (2008).

[12]. Wenzhong Ma E Jun Zhang E Xiaolin Wang, “ Formation of PVDF crystalline phases from THF/DMF mixed solvent”, Journal of Material Science, 43, 398-401, (2008).

[13]. Tawansi, A.; Oraby, A.H.; Abdelrazek, E.M.; Ayad, M. I.; Abdelaziz, M.; *“Journal of Applied Polymer Science”*, 70, 1437–1445, (1998).

[14]. Tawansi, A.; Oraby, A.H.; Ahmed, E.; Abdelrazek, E.M.; Abdelaziz, M.; *"Journal of Applied Polymer Science"*, 70, 1759, (1998).

[15]. Tawansi, A.; Oraby, A.H.; Abdelrazek, E.M.; Abdelaziz, M.; "Polymer Testing", 18, 569–579, (1999).

[16]. Tawansi, A.; Oraby, A.H.; Badar, S.I.; Abdelaziz, M.; "Journal of Material Science", 14,135-141, (2003).

[17]. Abdelazi, M.; Abdelrazek, E.M.; "Effect of equal amounts of Mn and Co dopant addition on the structural, electrical and magnetic properties of PVDF films", *Physica B* 349, 84-91, (2004).

[18]. Kumar, Neeraj.; Nath, R.; "Ferroelectric polarization switching in KNO3 : PVDF films", *J. Phys. D: Appl. Phys.* 36, 1308-1313, (2003).

[19]. Sekhar, K.C.; Nath, R.; "Study of ferroelectric properties in sodium nitrate; PVDF nanocomposites films", *Journal of applied physics* 102, 044114 (2007).

[20]. Nautiyal, Arvind.; Sekhar, K.C.; Pathak, N.P.; Nath, R.; "Ferroelectric and phase transition studies in cesium nitrate: PVDF composite films", Appl Phyc A, 97, 205-210 (2009).

[21]. El-Khodary, A.; Abdelaziz Gamal, M.; Hassan, M.; *"International Journal of Polymeric Materials"*, 54, 633–650, (2005).

[22]. Joao Sinezio de C. Campos.; Alexandre, A.; *"Materials science and engineering"*, 136,123-128, (2007).

[23]. Elashmawi, I.S.; "Effect of NaCl filler on ferroelectric phase and polaron configuration of PVDF films", *Cryst. Res. Technol,* 42, 389-393 (2007).

[24]. Elashmawi, I.S.; "Effect of LiCl filler on the structure and morphology of PVDF films", *Materials chemistry and physis* 107, 96-100, (2008).

[25]. T. Miyamoto, K. Shibayam, *J. Appl.* 44, 5372 (1973).

[26]. Y. Kamoto, T.F. Ychii, S. Lee, T.A. Skotheim, *J. Polym. Sci., Part A: Polym. Chem.* 31,2573 (1973).